TU/e EINDHOVEN UNIVERSITY OF TECHNOLOGY

Rigorous analysis of thick microstrip antennas and wire antennas embedded in a substrate

Citation for published version (APA):
Smolders, A. B. (1992). *Rigorous analysis of thick microstrip antennas and wire antennas embedded in a substrate*. (EUT report. E, Fac. of Electrical Engineering; Vol. 92-E-263). Eindhoven University of Technology.

Document status and date:
Published: 01/01/1992

Document Version:
Publisher's PDF, also known as Version of Record (includes final page, issue and volume numbers)

Please check the document version of this publication:

• A submitted manuscript is the version of the article upon submission and before peer-review. There can be important differences between the submitted version and the official published version of record. People interested in the research are advised to contact the author for the final version of the publication, or visit the DOI to the publisher's website.
• The final author version and the galley proof are versions of the publication after peer review.
• The final published version features the final layout of the paper including the volume, issue and page numbers.

Link to publication

General rights
Copyright and moral rights for the publications made accessible in the public portal are retained by the authors and/or other copyright owners and it is a condition of accessing publications that users recognise and abide by the legal requirements associated with these rights.

• Users may download and print one copy of any publication from the public portal for the purpose of private study or research.
• You may not further distribute the material or use it for any profit-making activity or commercial gain
• You may freely distribute the URL identifying the publication in the public portal.

If the publication is distributed under the terms of Article 25fa of the Dutch Copyright Act, indicated by the "Taverne" license above, please follow below link for the End User Agreement:

www.tue.nl/taverne

Take down policy
If you believe that this document breaches copyright please contact us at:

openaccess@tue.nl

providing details and we will investigate your claim.

Download date: 04. Oct. 2023

tu/e
Research Report
ISSN 0167-9708
Coden: TEUEDE

Eindhoven
University of Technology
Netherlands

Faculty of Electrical Engineering

Rigorous Analysis of Thick Microstrip Antennas and Wire Antennas Embedded in a Substrate

by
A.B. Smolders

EUT Report 92-E-263
ISBN 90-6144-263-X
july 1992

Eindhoven University of Technology Research Reports
EINDHOVEN UNIVERSITY OF TECHNOLOGY

Faculty of Electrical Engineering
Eindhoven The Netherlands

ISSN 0167-9708 Coden: TEUEDE

Rigorous Analysis of Thick Microstrip Antennas and Wire Antennas Embedded in a Substrate

by

A.B. Smolders

EUT Report 92-E-263
ISBN 90-6144-263-X

EINDHOVEN
JULY 1992

CIP-GEGEVENS KONINKLIJKE BIBLIOTHEEK, DEN HAAG

Smolders, A.B.

Rigorous analysis of thick microstrip antennas and wire antennas embedded in a substrate / by A.B. Smolders. - Eindhoven : Eindhoven University of Technology, Faculty of Electrical Engineering. - Fig. - (EUT report, ISSN 0167-9708 ; 92-E-263)
Met lit. opg., reg.
ISBN 90-6144-263-X
NUGI 832
Trefw.: microstripantennes.

Abstract

In this report an efficient yet rigorous method is presented for the analysis of electrically thick rectangular microstrip antennas and wire antennas with a dielectric cover. The method of moments is used in combination with the exact spectral domain Green's function in order to find the unknown currents on the antenna. The microstrip antenna is fed by a coaxial cable. A proper model of the feeding coaxial structure is used. In addition, a special attachment mode has been applied to ensure continuity of current at the patch-coax transition. The effieciency of the method of moments is improved by using the so called source term extraction technique, where a great part of the infinite integrals involved with the method of moment formulation is calculated analytically. Furthermore, computation time can be saved by selecting a set of basis functions that describes the current distribution on the patch and probe in an accurate way using only a few terms of this set. Thick microstrip antennas have broadband characteristics. However, a proper match to 50 Ω is often difficult. This matching problem can be avoided by using a slightly different excitation structure. The patch is now electromagnetically coupled to the feeding probe. A bandwidth of more than 40 percent ($VSWR < 2$) can easily be obtained for this type of microstrip antenna. The price that has to be paid is a degradation of the radiation characteristics.

Smolders, A.B.
RIGOROUS ANALYSIS OF THICK MICROSTRIP ANTENNAS AND WIRE ANTENNAS EMBEDDED IN A SUBSTRATE.
Faculty of Electrical Engineering, Eindhoven University of Technology,
The Netherlands, 1992.
EUT Report 92-E-263, ISBN 90-6144-263-X

Address of the author
Electromagnetics Division
Faculty of Electrical Engineering, Eindhoven University of Technology
P.O. Box 513
5600 MB Eindhoven
The Netherlands

Acknowledgements

This research was supported by the Technology foundation (STW). The author wishes to thank Prof. J. Boersma for his contribution to the calculation of some of the infinite integrals of chapter 2. The author also wishes to acknowledge Dr. M.E.J. Jeuken for the many helpful discussions.

Contents

Chapter 1

Introduction

Over the past decade, microstrip antennas and -array's have become quite popular owing to features such as light weight, conformalibility and potentially low production costs. There are many applications for microstrip antennas ranging from mobile communications to phased array radar systems. Due to the planar structure of microstrip antennas, it is possible to integrate the active devices together with the feeding network and radiating elements. This can also reduce production costs significantly, especially for large volume production. For some of these applications a bandwidth of only a few percent is required. However, in most practical applications a larger bandwidth is required. For mobile satellite communication a bandwidth of at least 6.5 percent is needed whereas for certain radar systems bandwidth requirements of more then 40 percent can be expected.

In figure 1.1 the side view is shown of a single microstrip antenna. The antenna consists of a groundplane covered with a dielectric substrate. The patch is located in or on the dielectric and is fed by a coaxial cable. Other excitation principles are also possible - a microstrip line, for example.

One way to improve the bandwidth of a microstrip element is by using a thicker substrate. Another way to improve the bandwidth of a microstrip antenna is by using capacitive elements above the patch (stacked structure) or parallel to the patch (gap-coupled structure). In this report we have chosen for the first option, that is, bandwidth improvement by using an electrically thick dielectric substrate. In order to be able to analyse electrically thick microstrip antennas fed by a coaxial cable, a rigorous model has to be used. The thickness of the antenna and the presence of the feeding probe (often neglected in simple models) have to be incorporated in the analysis. Therefore we shall use the method of moments for the analysis of thick microstrip antennas. This approach uses the exact spectral domain Green's function, which implies that all effects are included. In [1,7,8] this method has been applied to electrically thin microstrip antennas, where the presence of the feeding probe can be neglected.

Usually one is interested not only in the performance of a single isolated microstrip antenna, but in array's of microstrip antennas. So it is very important that the computation time involved with a rigorous analysis of one single thick microstrip antenna is minimized.

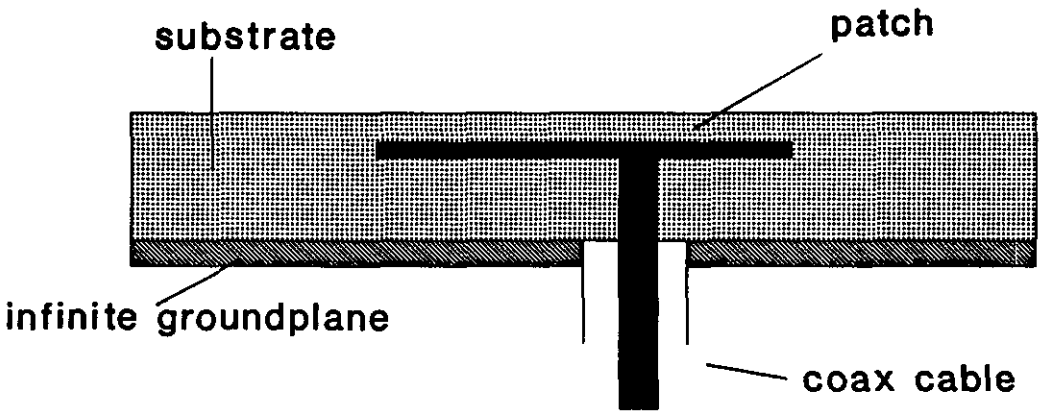

Figure 1.1: Microstrip antenna fed by a coaxial cable (side view)

We have therefore chosen for a set of basis functions that describes the current distribution on the patch and probe in an accurate way, using only a few basis functions of this set. Furthermore a special attachment mode is used at the patch-probe transition to ensure continuity of current. In addition to this, special analytical and numerical techniques have to be used to reduce the computation time needed to evaluate the infinite integrals involved with the method of moments formulation [4].

The organisation of this report is as follows. First a proper model of the feeding coaxial structure is discussed. Therefore a wire antenna embedded in a dielectric substrate above a infinite groundplane is investigated. In fact, this chapter serves as an introduction to chapter 3, where a rigorous method for the analysis of electrically thick microstrip antennas is presented. Some applications of this model with broadband characteristics shall be discussed. And finally, in chapter 4 the far field pattern of thick microstrip antennas is investigated.

Chapter 2

Analysis of a wire antenna embedded in a substrate above a groundplane using a spectral domain moment method

2.1 Introduction

We will consider the wire antenna here because it serves as an introduction for the rigorous analyses of probe-fed thick microstrip antennas. A lot of research has already been performed on wire antennas in free space using different types of models. We have checked the correctness of our method with these models.

2.2 Model description

We will assume that the current distribution is located at the outer surface of the perfectly conducting wire. We will also assume that this surface current has no component in the ϕ direction, i.e.

$$\vec{J}_s = \frac{I(z)}{2\pi a}\vec{e}_z \tag{2.1}$$

In figure 2.1 the geometry of the structure is shown. The wire antenna has a diameter 2a and is located in a substrate with a permittivity ϵ_r above a perfectly conducting infinite groundplane. The antenna is fed by a coaxial cable with inner diameter 2a and outer diameter 2b.
The wire antenna is excited by the fields in the coaxial aperture. At frequencies for which $kb < 0.1$, the fields in the coaxial aperture can be modelled by the fields corresponding to

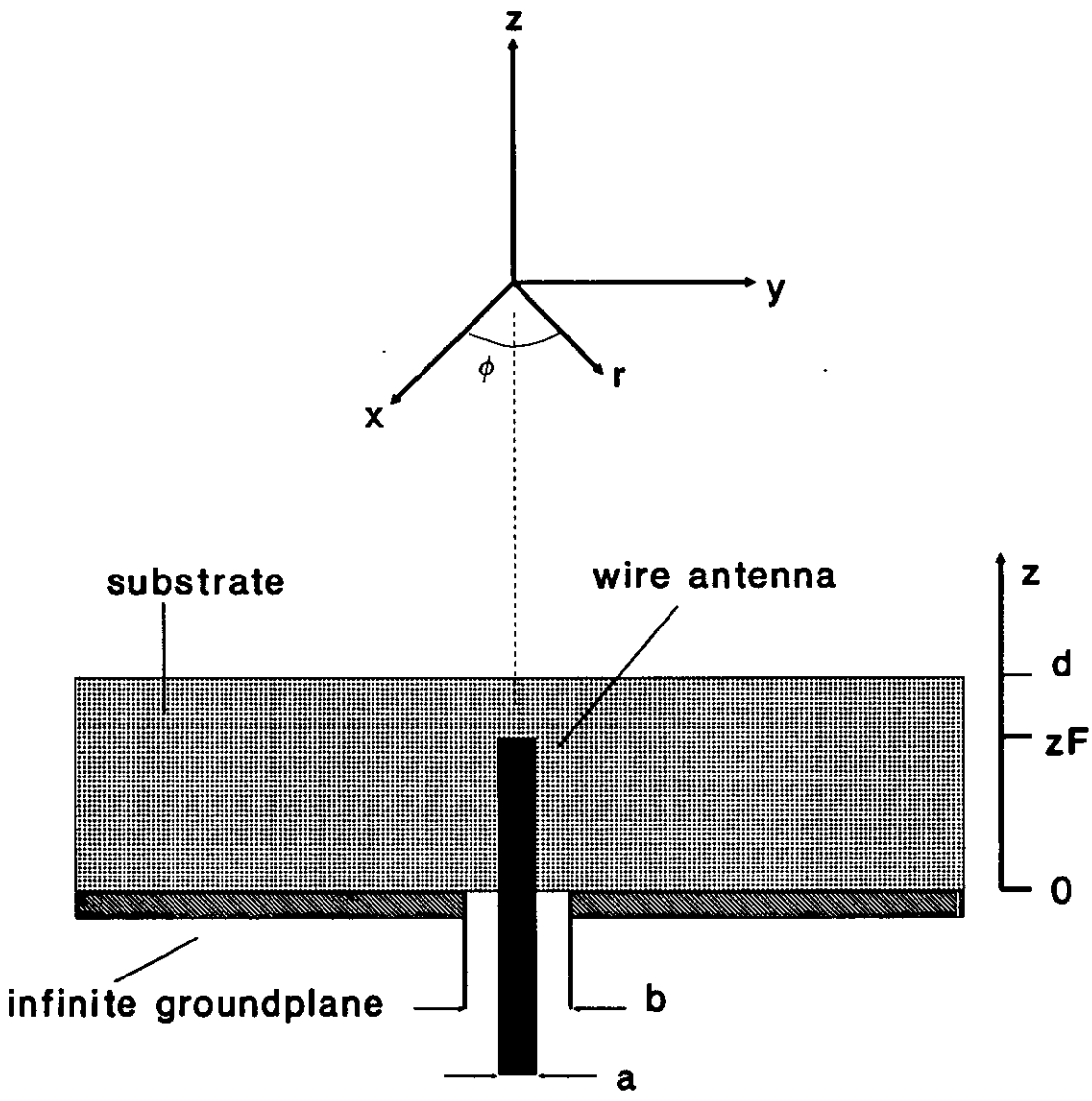

Figure 2.1: Wire antenna embedded in a substrate (side view)

the groundmode, i.e. the TEM-mode. The fields in the aperture then take the form (z=0):

$$\begin{aligned}\vec{\mathcal{E}}_r(r) &\approx \vec{\mathcal{E}}_{rTEM}(r) = \frac{V}{r ln(\frac{b}{a})}\vec{e}_r \quad a \leq r \leq b \\ \vec{\mathcal{H}}_\phi(r) &\approx \vec{\mathcal{H}}_{\phi TEM}(r) = \frac{I}{2\pi r}\vec{e}_\phi \quad a \leq r \leq b\end{aligned} \tag{2.2}$$

Where V is the voltage between the inner and outer conductor of the coaxial cable and I is the total current at the base (z=0) of the wire antenna. Note that the base current I has to be calculated. Ones I is known the input impedance of the antenna can be determined with the simple formula:

$$Z_{in} = \frac{V}{I(z=0)} \tag{2.3}$$

In our model the electric field in the coaxial aperture is used as a source. This source can also be modelled by a magnetic current distribution in the aperture of the coax:

$$\vec{\mathcal{M}} = \mathcal{M}_\phi \vec{e}_\phi = \vec{\mathcal{E}}_r \times \vec{e}_z = -\frac{V}{r ln(\frac{b}{a})}\vec{e}_\phi \tag{2.4}$$

In literature this source model is often called the "Magnetic frill excitation model".

2.3 Green's function of a $\hat{z}$-directed dipole

In [1] the Green's function of an $\hat{x}$- and $\hat{y}$-directed dipole embedded in a substrate above an infinite groundplane was calculated in the spectral domain. In this section the spectral domain Green's function of a $\hat{z}$-directed dipole is determined. In figure 2.2 the geometry of the layered structure is shown.
The dipole is located at the point (x_0, y_0, z_0). We shall now trie to find the fields at (x,y,z) due to the vertical dipole. With a time-dependence $e^{j\omega t}$, Maxwell's equations take the form:

$$\begin{aligned}\nabla \times \vec{\mathcal{E}} &= -j\omega\mu_0\vec{\mathcal{H}} \\ \nabla \times \vec{\mathcal{H}} &= j\omega\epsilon\vec{\mathcal{E}} + \vec{\mathcal{J}}\end{aligned} \tag{2.5}$$

ω is the radial frequency, ϵ the permittivity and μ_0 the permeability of the medium under consideration. $\vec{\mathcal{J}}$ is the current density in the medium. The electric and magnetic fields can be expressed in terms of the vector potential $\vec{A}$ and scalar potential ϕ:

$$\begin{aligned}\vec{\mathcal{H}} &= \frac{1}{\mu_0}\nabla \times \vec{A} \\ \vec{\mathcal{E}} &= -j\omega\vec{A} - \nabla\phi\end{aligned} \tag{2.6}$$

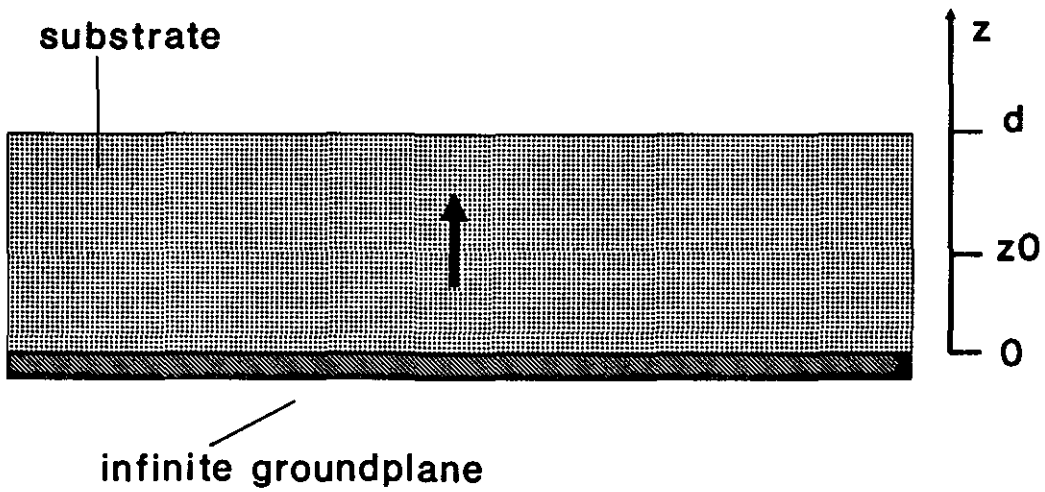

Figure 2.2: Vertical electric dipole in a substrate above a groundplane

The divergence of the vector potential $\vec{A}$ can be specified with the Lorentz gauge:

$$\nabla.\vec{A} = -j\omega\epsilon\mu_0\phi \tag{2.7}$$

This results in the following expression for the electric and magnitic fields:

$$\begin{aligned}\vec{\mathcal{E}} &= -\frac{j\omega}{k^2}[k^2\vec{A} + \nabla(\nabla.\vec{A})] \\ \vec{\mathcal{H}} &= \frac{1}{\mu_0}\nabla \times \vec{A}\end{aligned} \tag{2.8}$$

In the above expression the wavenumber $k = \omega\sqrt{\epsilon\mu_0}$ is used. Substituting the above expression in Maxwell's equations (2.5), results in the Helmholtz equation for the vector potential $\vec{A}$:

$$\nabla^2\vec{A} + k^2\vec{A} = -\mu_0\vec{\mathcal{J}} \tag{2.9}$$

The vector potential can be expressed in terms of the dyadic Green's function:

$$\vec{A}(\vec{r}) = \int\int\int \bar{\bar{\mathcal{G}}}(\vec{r},\vec{r}_0).\vec{\mathcal{J}}(r_0)\, dV_0 \tag{2.10}$$

In order to solve the boundary value problem, we have to apply the boundary conditions of the fields at the z=0 and z=d plane. Fields in the substrate (=region 1) are indicated with

an index 1 and fields in free space (region 2) are indicated by an index 2. The boundary conditions can then be written in the form:

$$\begin{aligned} z = 0 \ plane: &\quad \vec{e}_z \times \vec{\mathcal{E}}_1 = \vec{0} \\ z = d \ plane: &\quad \vec{e}_z \times \vec{\mathcal{E}}_1 = \vec{e}_z \times \vec{\mathcal{E}}_2 \\ &\quad \vec{e}_z \times \vec{\mathcal{H}}_1 = \vec{e}_z \times \vec{\mathcal{H}}_2 \end{aligned} \tag{2.11}$$

It is not possible to find a closed form expression for the vector potential in the space (x,y,z) domain. In the spectral domain however, a solution for the above boundary value problem can be easily obtained. We shall therefore transform all quantities to the spectral domain. For a general function F(x,y) the Fourier transform and it's corresponding inverse Fourier transform are defined as:

$$\begin{aligned} F(k_x, k_y) &= \int\int \mathcal{F}(x,y) e^{jk_x x} e^{jk_y y} \, dxdy \\ \mathcal{F}(x,y) &= \frac{1}{4\pi^2} \int\int F(k_x, k_y) e^{-jk_x x} e^{-jk_y y} \, dk_x dk_y \end{aligned} \tag{2.12}$$

If we choose $\mathcal{A}_{1x} = \mathcal{A}_{1y} = \mathcal{A}_{2x} = \mathcal{A}_{2y} = 0$, we finally find the vector potential in medium 1 due to a $\hat{z}$ -directed dipole:

$$A_{1z} = G_{1zz} = \mu_0 e^{jk_x x_0} e^{jk_y y_0} \begin{cases} -\dfrac{\cos k_1 z}{k_1} \left[\sin k_1 z_0 + j \dfrac{Nm}{Tm} \cos k_1 z_0 \right] & 0 \le z \le z_0 \\ -\dfrac{\cos k_1 z_0}{k_1} \left[\sin k_1 z + j \dfrac{Nm}{Tm} \cos k_1 z \right] & z_0 \le z \le d \end{cases} \tag{2.13}$$

With

$$\begin{aligned} Nm &= k_1 \cos k_1 d + j k_2 \epsilon_r \sin k_1 d \\ Tm &= k_2 \epsilon_r \cos k_1 d + j k_1 \sin k_1 d \\ k_1^2 &= \epsilon_r k_0^2 - k_x^2 - k_y^2 \qquad (Im(k_1) < 0) \\ k_2^2 &= k_0^2 - k_x^2 - k_y^2 \qquad (Im(k_2) < 0) \end{aligned}$$

The spectral coordinates (k_x, k_y) can also be written in terms of polar coordinates:

$$k_x = k_0 \beta \cos\alpha \quad k_y = k_0 \beta \sin\alpha$$

The above expression can also be written in the form:

$$G_{1zz} = \mu_0 e^{jk_x x_0} e^{jk_y y_0} \begin{cases} \dfrac{\cos k_1 z}{k_1 Tm} \left[\epsilon_r k_2 \sin k_1 (d - z_0) - j k_1 \cos k_1 (d - z_0) \right] & 0 \le z \le z_0 \\ \dfrac{\cos k_1 z_0}{k_1 Tm} \left[\epsilon_r k_2 \sin k_1 (d - z) - j k_1 \cos k_1 (d - z) \right] & z_0 \le z \le d \end{cases}$$

(2.14)

If we want to find an expression for the electric and magnetic fields due to a $\hat{z}$ -directed dipole we have to be careful in determining the z-component of the electric field. Let

$$G_{1zz} = G_3 \mu_0 e^{jk_x x_0} e^{jk_y y_0} \tag{2.15}$$

Then according to equation (2.8) and (2.10), the z- component of the electric field in the substrate due to a $\hat{z}$ -directed dipole can be written as:

$$E_{1z} = \frac{-j\omega\mu_0}{k^2} \left(k^2 G_3 + \partial_z{}^2 G_3\right) e^{jk_x x_0} e^{jk_y y_0} \tag{2.16}$$

The difficulty in determining E_{1z} is now that $\partial_z G_3$ has a discontinuity for $z = z_0$. This implies that the second derivative $\partial_z{}^2 G_3$ contains a δ function. Thus:

$$\partial_z{}^2 G_3 = -\delta(z - z_0) - k_1{}^2 G_3 \tag{2.17}$$

Combining the preceeding equations results in:

$$\begin{aligned} E_{1z} &= \frac{-j\omega\mu_0}{k^2} \left((k^2 - k_1{}^2) G_3 - \delta(z - z_0)\right) e^{jk_x x_0} e^{jk_y y_0} \\ &= Q_{zz} e^{jk_x x_0} e^{jk_y y_0} \end{aligned} \tag{2.18}$$

The other components of the electric field and the three components of the magnetic field in the spectral domain can be obtained without any difficulties:

$$\begin{aligned} E_{1x} &= \frac{-j\omega\mu_0}{k^2} \left(-jk_x \partial_z G_3\right) e^{jk_x x_0} e^{jk_y y_0} \\ &= Q_{xz} e^{jk_x x_0} e^{jk_y y_0} \\ E_{1y} &= \frac{-j\omega\mu_0}{k^2} \left(-jk_y \partial_z G_3\right) e^{jk_x x_0} e^{jk_y y_0} \\ &= Q_{yz} e^{jk_x x_0} e^{jk_y y_0} \end{aligned} \tag{2.19}$$

$$\begin{aligned} H_{1x} &= -jk_y G_3 e^{jk_x x_0} e^{jk_y y_0} \\ &= Q_{hxz} e^{jk_x x_0} e^{jk_y y_0} \\ H_{1y} &= jk_x G_3 e^{jk_x x_0} e^{jk_y y_0} \\ &= Q_{hyz} e^{jk_x x_0} e^{jk_y y_0} \\ H_{1z} &= Q_{hzz} = 0 \end{aligned} \tag{2.20}$$

For a general $\hat{z}$ -directed current distribution in the substrate the electric and magnetic fields in the substrate can be expressed in terms of the Fourier transform of this current distribution:

$$\vec{\mathcal{E}}_1(x, y, z) = \frac{1}{4\pi^2} \int_{-\infty}^{\infty} \int_{-\infty}^{\infty} \int_{z_0} \bar{\bar{Q}}(k_x, k_y, z_0, z) . J_z(k_x, k_y, z_0) \vec{e}_z dz_0 e^{-jk_x x} e^{-jk_y y} dk_x dk_y$$

With:

$$\bar{\bar{Q}}(k_x, k_y, z_0, z) = \begin{pmatrix} 0 & 0 & Q_{xz} \\ 0 & 0 & Q_{yz} \\ 0 & 0 & Q_{zz} \end{pmatrix} \tag{2.21}$$

and

$$\vec{\mathcal{H}}_1(x, y, z) = \frac{1}{4\pi^2} \int_{-\infty}^{\infty} \int_{-\infty}^{\infty} \int_{z_0} \bar{\bar{Q}}_h(k_x, k_y, z_0, z).J_z(k_x, k_y, z_0)\vec{e}_z dz_0 e^{-jk_x x} e^{-jk_y y} dk_x dk_y$$

With:

$$\bar{\bar{Q}}_h(k_x, k_y, z_0, z) = \begin{pmatrix} 0 & 0 & Q_{hxz} \\ 0 & 0 & Q_{hyz} \\ 0 & 0 & 0 \end{pmatrix} \tag{2.22}$$

$J_z(k_x, k_y, z_0)\vec{e}_z$ is the Fourier transform of the $\hat{z}$ -directed current density $J_z(x_0, y_0, z_0)\vec{e}_z$. Note that the zero elements in (2.21) and (2.22) are not equal to zero for a general current distribution in the substrate. In chapter 3 the other elements of these two matrices will also be defined.

2.4 Calculation of the current distribution on the wire antenna

2.4.1 Moment method formulation

On the outer surface of the wire antenna (r=a) the total tangentiel electric field has to be zero. The total electric field can be divided in two parts, i.e. a component due to the currents on the wire ($\vec{\mathcal{E}}_{wire}$) and a component due to the magnetic current in the coaxial aperture ($\vec{\mathcal{E}}_{frill}$). The boundary condition on the outer surface of the wire now takes the form:

$$\vec{n} \times (\vec{\mathcal{E}}_{wire} + \vec{\mathcal{E}}_{frill}) = \vec{0} \quad for \quad r = a \tag{2.23}$$

The next step in the method of moments formulation is the expansion of the unknown current on the wire in basis functions:

$$\vec{\mathcal{J}}_z(\vec{r_0}) = \vec{e}_z \mathcal{J}_z(\vec{r_0}) = \sum_{n=1}^{\infty} I_n \vec{\mathcal{J}}_{zn}(\vec{r_0}) \tag{2.24}$$

$\vec{\mathcal{E}}_{wire}$ can then be written as:

$$\begin{aligned}\vec{\mathcal{E}}_{wire}(\vec{r}) &= -\frac{j\omega}{k^2}(k^2+\nabla\nabla.)\vec{\mathcal{A}}_{wire}(\vec{r}) \\ &= -\frac{j\omega}{k^2}(k^2+\nabla\nabla.)\int\int_{wire}\bar{\bar{\mathcal{G}}}(\vec{r},\vec{r}_0).\vec{\mathcal{J}}(\vec{r}_0)\,dS_0 \\ &= -\frac{j\omega}{k^2}(k^2+\nabla\nabla.)\int\int_{wire}\bar{\bar{\mathcal{G}}}(\vec{r},\vec{r}_0).\sum_{n=1}^{\infty}I_n\vec{\mathcal{J}}_{zn}(\vec{r}_0)\,dS_0 \\ &= \sum_{n=1}^{\infty}I_n\vec{\mathcal{E}}_{nwire}(\vec{r})\end{aligned} \tag{2.25}$$

Substituting the above expression in (2.23) gives:

$$\vec{n}\times(\sum_{n=1}^{\infty}I_n\vec{\mathcal{E}}_{nwire}+\vec{\mathcal{E}}_{frill})=\vec{0}\quad for\quad r=a \tag{2.26}$$

Introduce a residue according to:

$$\vec{R}=\vec{n}\times(\sum_{n=1}^{\infty}I_n\vec{\mathcal{E}}_{nwire}+\vec{\mathcal{E}}_{frill})\doteq\vec{0}\quad for\quad r=a \tag{2.27}$$

Fysically the above equation has to be satisfied at all points on the outer surface of wire. We shall relax this condition a little bit. The residue is *weighted to zero* with weighting functions $\vec{\mathcal{J}}_{zm}$:

$$\langle\vec{R}\;;\;\vec{\mathcal{J}}_{zm}\rangle_{Sm}=\int\int_{Sm}\vec{R}.\vec{\mathcal{J}}_{zm}\,dSm=0\quad for\quad m=1,2... \tag{2.28}$$

Where S_m is the region on the wire for which weighting function $\vec{\mathcal{J}}_{zm}$ is unequal zero. This then results in a set of linear equations:

$$\sum_{n=1}^{\infty}I_n\int\int_{Sm}\vec{\mathcal{E}}_{nwire}.\vec{\mathcal{J}}_{zm}\,dSm+\int\int_{Sm}\vec{\mathcal{E}}_{frill}.\vec{\mathcal{J}}_{zm}\,dSm=0\quad for\quad m=1,2... \tag{2.29}$$

This set of equations can be written in the well known form:

$$\sum_{n=1}^{\infty}I_nZ_{mn}^{zz}+V_m^z=0\quad for\quad m=1,2...$$

or

$$[Z^{zz}][I]+[V^z]=[0] \tag{2.30}$$

with

$$\begin{aligned}Z_{mn}^{zz} &= 4\pi^2\int\int_{Sm}\vec{\mathcal{E}}_{nwire}(x,y,z).\vec{\mathcal{J}}_{zm}(z)\,dSm \\ V_m^z &= 4\pi^2\int\int_{Sm}\vec{\mathcal{E}}_{frill}(x,y,z).\vec{\mathcal{J}}_{zm}(z)\,dSm \\ &= -4\pi^2\int\int_{frill}\vec{\mathcal{H}}_{mwire}(x,y,0).\vec{\mathcal{M}}_{frill}(x,y,0)\,dxdy\end{aligned} \tag{2.31}$$

In order to rewrite an element of the excitation vector $[V^z]$ in terms of the magnetic current distribution in the coaxial aperture $\vec{\mathcal{M}}_{frill}$, the reaction concept is used [2]. In the above formulation we have used the same type of basis functions for expansion as well as for testing. This choice is known as a Galerkin moment method solution, which ensures a fast convergence [3]. Once the elements of $[Z^{zz}]$ and $[V^z]$ are known, the unknown mode coefficients [I] can be determined by solving matrix equation (2.30). The time needed to solve this matrix equation can usually be neglected compared with the time needed to calculate the elements of $[Z^{zz}]$ and $[V^z]$.

2.4.2 Basis functions on the wire antenna

In section 2.2 it is stated that it is assumed that the current on the wire antenna has no ϕ-component and depends only on the z-coordinate along the wire. In order to describe the current on the outer surface of the wire, we will expand this current in piece-wise linear basis functions, better known as rooftop basis functions.

$$\vec{\mathcal{J}}_{zn}(x,y,z) = \frac{1}{2\pi a}\delta(r-a)g_n(z)\vec{e}_z \tag{2.32}$$

with

$$g_n(z) = \begin{cases} \frac{2}{h}(\frac{h}{2}-z) & n=1 \quad 0 \le z \le \frac{h}{2} \\ \frac{2}{h}(z-z_{n-1}) & n \ge 2 \quad z_{n-1} \le z \le z_n \\ \frac{2}{h}(z_{n+1}-z) & n \ge 2 \quad z_n \le z \le z_{n+1} \end{cases}$$

In figure 2.3 the z-dependent part of the basis functions is shown. The total number of basis functions on the wire is N_z.
Note that the condition $\vec{\mathcal{J}}_z(z=z_F) = \vec{0}$ is satisfied through the choice of the last basis function ($n = N_z$). All calculations are performed in the spectral domain. Therefore we have to know the Fourier transform of (2.32). Applying (2.12) then yields:

$$\vec{J}_{zn}(k_x,k_y,z) = J_0(k_0\beta a)g_n(z)\vec{e}_z \tag{2.33}$$

with $k_x^2 + k_y^2 = k_0^2\beta^2$. J_0 is the Bessel function of the first kind with order zero. Some authors assume for the sake of symplicity that the current distribution along the wire antenna is concentrated on the axis of the wire. Setting a=0 in the above expression gives the Fourier transform for this situation.

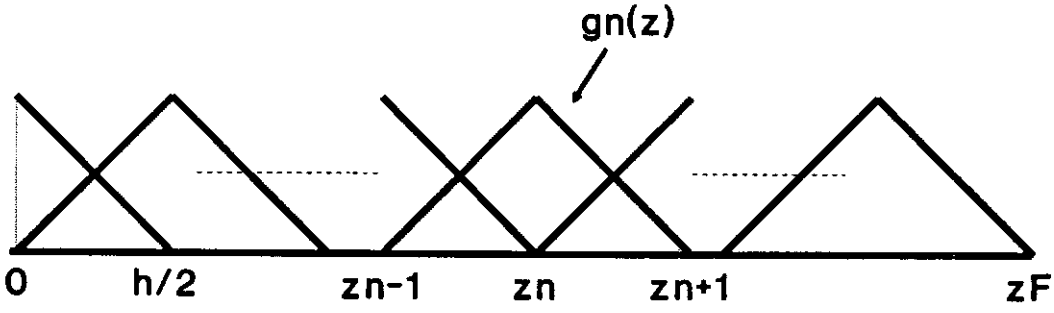

Figure 2.3: Rooftop basis functions along the wire antenna

2.5 Efficient evaluation of the matrix $[Z^{zz}]$

2.5.1 Introduction

An element of the matrix $[Z^{zz}]$ can be calculated by using expression (2.31). Because of the fact that the Green's function is known in closed form in the spectral domain (k_x, k_y, z) we shall rewrite this expression in terms of spectral domain quantities.

$$\begin{aligned} Z_{mn}^{zz} &= 4\pi^2 \int\int_{Sm} \vec{\mathcal{E}}_{nwire}(x,y,z).\vec{\mathcal{J}}_{zm}(x,y,z)\, dSm \\ &= 4\pi^2 \int\int_{Sm} \left[\frac{1}{4\pi^2}\int_{-\infty}^{\infty}\int_{-\infty}^{\infty}\int_{z_0} \bar{\bar{Q}}(k_x,k_y,z_0,z).\vec{J}_{zn}(k_x,k_y,z_0)dz_0 \right. \\ &\quad \left. e^{-jk_x x}e^{-jk_y y}dk_x dk_y\right] .\vec{\mathcal{J}}_{zm}(x,y,z)\, dSm \\ &= \int_{-\infty}^{\infty}\int_{-\infty}^{\infty}\int_z\int_{z_0} \bar{\bar{Q}}(k_x,k_y,z_0,z).\vec{J}_{zn}(k_x,k_y,z_0)dz_0 \\ &\quad .\left[\int_x\int_y \vec{\mathcal{J}}_{zm}(x,y,z)e^{-jk_x x}e^{-jk_y y}dxdy\right] dzdk_x dk_y \\ &= \int_{-\infty}^{\infty}\int_{-\infty}^{\infty}\int_z \left[\int_{z_0} \bar{\bar{Q}}(k_x,k_y,z_0,z).\vec{J}_{zn}(k_x,k_y,z_0)dz_0\right] .\vec{J}^{*}_{zm}(k_x,k_y,z)dzdk_x dk_y \end{aligned} \tag{2.34}$$

Relation (2.21) has been used in the above derivation. The above expression can be simplified by introducing a change to polar coordinates , i.e. $k_x = k_0\beta\cos\alpha$ and $k_y =$

$k_0\beta\sin\alpha$. Because both $\bar{\bar{Q}}$ as well as $\vec{J}_{zn}$ are α independent, an element of the matrix $[Z^{zz}]$ is given by:

$$Z_{mn}^{zz} = \int_0^\infty \int_z [\int_{z_0} \bar{\bar{Q}}(\beta, z_0, z).\vec{J}_{zn}(\beta, z_0)dz_0]\vec{J}_{zm}^*(\beta, z)k_0^2\beta dz d\beta \tag{2.35}$$

The two z integrations in (2.35) can be calculated analytically in the case of rooftop basis functions. This issue is discussed in the next section. After eliminating the z integrations, an element of the matrix $[Z^{zz}]$ can be expressed in terms of one infinite beta integral. The fact that only one integral remains in the final expression for Z_{mn}^{zz} is due to the radial symmetry of the problem. Because test- en expansion functions are the same, the matrix $[Z^{zz}]$ is symmetric. So only the elements of the lower triangle of $[Z^{zz}]$ have to be evaluated.

2.5.2 Analytical evaluation of the z-integrals

In this section the analytical results of the two z-integrations in expression (2.35) are presented. Calculation of these integrals by hand requires much paper and a lot of patience. Therefore we have used the computer algebra software package *Maple* in order to find an analytical solution for the two z-integrations. Consider an element Z_{mn}^{zz}. We can distinguish three situations

- $n = m$: selfterm.
- $n = m - 1$: subdomain m and subdomain n overlap each other.
- $n \leq m - 2$: subdomain m and subdomain n do not overlap each other.

Each of the three situations will be examined in more detail.

i. $n = m$

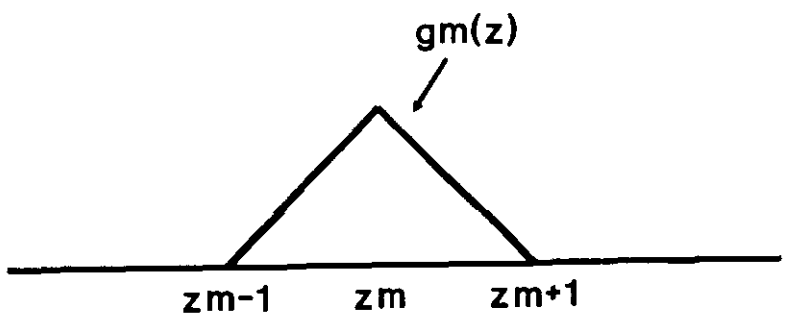

$$\begin{aligned} Z_{mm}^{zz} &= 2\pi \int_0^\infty \int_{z_{m-1}}^{z_{m+1}} [\int_{z_{m-1}}^{z_{m+1}} \bar{\bar{Q}}(\beta, z_0, z).\vec{J}_{zm}(\beta, z_0)dz_0]\vec{J}_{zm}^*(\beta, z)k_0^2\beta dz d\beta \\ &= 2\pi \int_0^\infty J_0^2(k_0\beta a)k_0^2\beta \int_{z_{m-1}}^{z_{m+1}} [\int_{z_{m-1}}^{z_{m+1}} \bar{\bar{Q}}(\beta, z_0, z).g_m(z_0)dz_0]g_m(z)dz d\beta \\ &= 2\pi \int_0^\infty J_0^2(k_0\beta a)k_0^2\beta I_{mm}^{zz}(\beta)d\beta \end{aligned} \tag{2.36}$$

with

$$
\begin{aligned}
I_{mm}^{zz} &= \int_{z_{m-1}}^{z_m} g_m(z) \left[\int_{z_{m-1}}^{z} g_m(z_0) Q_{zz}(z_0 < z) dz_0 \right. \\
&\left. + \int_{z}^{z_m} g_m(z_0) Q_{zz}(z_0 > z) dz_0 + \int_{z_m}^{z_{m+1}} g_m(z_0) Q_{zz}(z_0 > z) dz_0 \right] dz \\
&+ \int_{z_m}^{z_{m+1}} g_m(z) \left[\int_{z_{m-1}}^{z_m} g_m(z_0) Q_{zz}(z_0 < z) dz_0 \right. \\
&\left. + \int_{z_m}^{z} g_m(z_0) Q_{zz}(z_0 < z) dz_0 + \int_{z}^{z_{m+1}} g_m(z_0) Q_{zz}(z_0 > z) dz_0 \right] dz \\
&+ \frac{j\omega\mu_0}{\epsilon_r k_0^2} \int_{z_{m-1}}^{z_m} g_m(z) g_m(z_{m-1} \leq z \leq z_m) dz \\
&+ \frac{j\omega\mu_0}{\epsilon_r k_0^2} \int_{z_m}^{z_{m+1}} g_m(z) g_m(z_m \leq z \leq z_{m+1}) dz
\end{aligned}
$$

The last two terms in the above expression are due to the $\delta(z - z_0)$ term in Q_{zz} (see (2.18)). According to (2.18) $Q_{zz}(z_0 < z)$ and $Q_{zz}(z_0 > z)$ can be written as:

$$
Q_{zz}(z_0 < z) = \frac{-j\omega\mu_0 k_0^2 \beta^2 \cos k_1 z_0}{k^2 k_1 Tm} \left[\epsilon_r k_2 \sin k_1(d - z) - j k_1 \cos k_1(d - z) \right]
$$

$$
Q_{zz}(z_0 > z) = \frac{-j\omega\mu_0 k_0^2 \beta^2 \cos k_1 z}{k^2 k_1 Tm} \left[\epsilon_r k_2 \sin k_1(d - z_0) - j k_1 \cos k_1(d - z_0) \right]
$$

Substitute the above relations in (2.36) and use $g_m(z)$ according to (2.32). After performing the two z integrations analytically the final expression for I_{mm}^{zz} takes the form for $m > 1$:

$$
\begin{aligned}
I_{mm}^{zz} &= \frac{j\omega\mu_0}{\epsilon_r} \left\{ \left(-\frac{h\epsilon_r}{3k_0^2(\beta^2 - \epsilon_r)} + \frac{4\beta^2}{hk_1^2} \right) \epsilon_m - \frac{4\beta^2}{h^2 k_1^5 Tm} \right. \\
&\quad [\epsilon_r k_2 (\cos k_1 z_{m-1} \sin k_1(d - z_{m-1}) - 4 \cos k_1 z_{m-1} \sin k_1(d - z_m) \\
&\quad + 2 \cos k_1 z_{m-1} \sin k_1(d - z_{m+1}) + 4 \cos k_1 z_m \sin k_1(d - z_m) \\
&\quad - 4 \cos k_1 z_m \sin k_1(d - z_{m+1}) + \cos k_1 z_{m+1} \sin k_1(d - z_{m+1})) \\
&\quad - j k_1 (\cos k_1 z_{m-1} \cos k_1(d - z_{m-1}) - 4 \cos k_1 z_{m-1} \cos k_1(d - z_m) \\
&\quad + 2 \cos k_1 z_{m-1} \cos k_1(d - z_{m+1}) + 4 \cos k_1 z_m \cos k_1(d - z_m) \\
&\quad \left. - 4 \cos k_1 z_m \cos k_1(d - z_{m+1}) + \cos k_1 z_{m+1} \cos k_1(d - z_{m+1})) \right] \}
\end{aligned}
\tag{2.37}
$$

With $\epsilon_m = 1$ for $m \geq 2$ and $\epsilon_m = \frac{1}{2}$ for $m = 1$. In the m=1 case (half rooftop basis function) z_m and z_{m-1} should be set to zero.

ii. $n = m - 1$

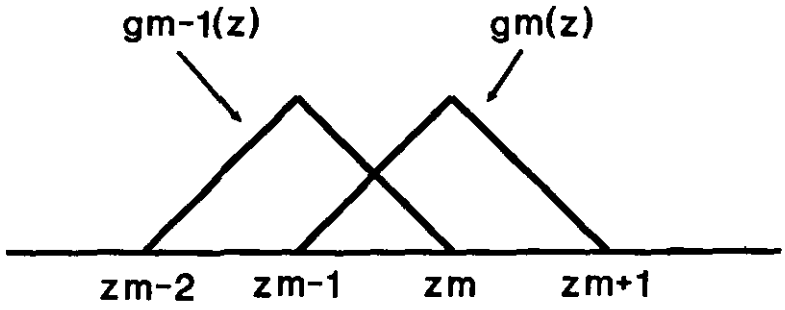

$$Z^{zz}_{mm-1} = 2\pi \int_0^\infty J_0^2(k_0\beta a)k_0^2\beta I^{zz}_{mm-1}(\beta)d\beta \tag{2.38}$$

with

$$\begin{aligned}
I^{zz}_{mm-1} &= \int_{z_{m-1}}^{z_m} g_m(z)\left[\int_{z_{m-2}}^{z_{m-1}} g_{m-1}(z_0)Q_{zz}(z_0 < z)dz_0\right. \\
&\left. + \int_{z_{m-1}}^{z} g_{m-1}(z_0)Q_{zz}(z_0 < z)dz_0 + \int_{z}^{z_m} g_{m-1}(z_0)Q_{zz}(z_0 > z)dz_0\right] dz \\
&+ \int_{z_m}^{z_{m+1}} g_m(z)\left[\int_{z_{m-2}}^{z_{m-1}} g_{m-1}(z_0)Q_{zz}(z_0 < z)dz_0\right. \\
&\left. + \int_{z_{m-1}}^{z_m} g_{m-1}(z_0)Q_{zz}(z_0 < z)dz_0\right] dz \\
&+ \frac{j\omega\mu_0}{\epsilon_r k_0^2}\int_{z_{m-1}}^{z_m} g_m(z)g_{m-1}(z_{m-1} \le z \le z_m)dz
\end{aligned}$$

The last term in the above expression is due to the $\delta(z - z_0)$ term in Q_{zz} (see (2.18)). Performing the z integrations analytically yields:

$$\begin{aligned}
I^{zz}_{mm-1} &= \frac{j\omega\mu_0}{\epsilon_r}\left\{\left(-\frac{h\epsilon_r}{12k_0^2(\beta^2 - \epsilon_r)} - \frac{2\beta^2}{hk_1^2}\right) - \frac{4\beta^2}{h^2k_1^5Tm}\right. \\
&[\epsilon_r k_2 (\cos k_1 z_{m-2} \sin k_1(d - z_{m-1}) - 2\cos k_1 z_{m-2} \sin k_1(d - z_m) \\
&+ \cos k_1 z_{m-2} \sin k_1(d - z_{m+1}) + 5\cos k_1 z_{m-1} \sin k_1(d - z_m) \\
&-2\cos k_1 z_{m-1} \sin k_1(d - z_{m-1}) - 2\cos k_1 z_{m-1} \sin k_1(d - z_{m+1}) \\
&-2\cos k_1 z_m \sin k_1(d - z_m) + \cos k_1 z_m \sin k_1(d - z_{m+1})) \\
&-jk_1 (\cos k_1 z_{m-2} \cos k_1(d - z_{m-1}) - 2\cos k_1 z_{m-2} \cos k_1(d - z_m) \\
&+ \cos k_1 z_{m-2} \cos k_1(d - z_{m+1}) + 5\cos k_1 z_{m-1} \cos k_1(d - z_m) \\
&-2\cos k_1 z_{m-1} \cos k_1(d - z_{m-1}) - 2\cos k_1 z_{m-1} \cos k_1(d - z_{m+1}) \\
&\left.-2\cos k_1 z_m \cos k_1(d - z_m) + \cos k_1 z_m \cos k_1(d - z_{m+1}))]\right\}
\end{aligned} \tag{2.39}$$

If $m-1=1$, i.e. $m=2$, z_{m-2} and z_{m-1} should be set to zero.

iii. $n \leq m-2$

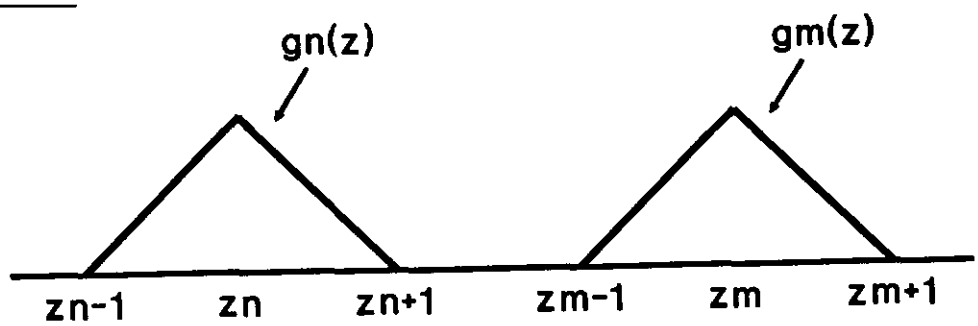

$$Z_{mn}^{zz} = 2\pi \int_0^\infty J_0^2(k_0\beta a) k_0^2 \beta I_{mn}^{zz}(\beta) d\beta \tag{2.40}$$

with

$$\begin{aligned} I_{mn}^{zz} &= \int_{z_{m-1}}^{z_m} g_m(z) \left[\int_{z_{n-1}}^{z_n} g_n(z_0) Q_{zz}(z_0 < z) dz_0 \right. \\ &\quad \left. + \int_{z_n}^{z_{n+1}} g_n(z_0) Q_{zz}(z_0 < z) dz_0 \right] dz \\ &\quad + \int_{z_m}^{z_{m+1}} g_m(z) \left[\int_{z_{n-1}}^{z_n} g_n(z_0) Q_{zz}(z_0 < z) dz_0 \right. \\ &\quad \left. + \int_{z_n}^{z_{n+1}} g_n(z_0) Q_{zz}(z_0 < z) dz_0 \right] dz \end{aligned}$$

Performing the z integrations analytically one obtains:

$$\begin{aligned} I_{mn}^{zz} &= -\frac{j\omega\mu_0}{\epsilon_r} \frac{4\beta^2}{h^2 k_1^5 Tm} [2\cos k_1 z_n - \cos k_1 z_{n-1} - \cos k_1 z_{n+1}] \\ &\quad [\, \epsilon_r k_2 (2\sin k_1(d-z_m) - \sin k_1(d-z_{m-1}) - \sin k_1(d-z_{m+1})) \\ &\quad -jk_1 (2\cos k_1(d-z_m) - \cos k_1(d-z_{m-1}) - \cos k_1(d-z_{m+1}))] \end{aligned} \tag{2.41}$$

If $n=1$, z_n and z_{n-1} should be set to zero.

2.5.3 Improved computational efficiency: source term extraction

The evaluation of the infinite β integrals is from a numerical point of view very time consuming. Especially if subdomain m touches or overlaps subdomain n. Therefore we

shall use the technique of [4] to improve the computational efficiency. Using this so called *source term extraction technique* the asymptotic form of the β integrand is subtracted from the original integrand, resulting in a fast converging integral. The infinite integration over the asymptotic form of the integrand can be calculated analytically. Other numerical problems associated with the evaluation of the infinite integral (for example poles due to surface waves) have already been discussed in [1], [4]. The reader is referred to these previous reports for more details.
If $I^{zz}_{Hmn}(\beta)$ is the asymptotic form of $I^{zz}_{mn}(\beta)$ then the source term extracting technique in formula form reads:

$$\begin{aligned} Z^{zz}_{mn} &= 2\pi \int_0^\infty J_0^2(k_0\beta a) k_0^2 \beta I^{zz}_{mn}(\beta) d\beta \\ &= 2\pi \int_0^v J_0^2(k_0\beta a) k_0^2 \beta I^{zz}_{mn}(\beta) d\beta \\ &+2\pi \int_v^\infty J_0^2(k_0\beta a) k_0^2 \beta (\ I^{zz}_{mn}(\beta) - I^{zz}_{Hmn}(\beta)\ ) d\beta \\ &+2\pi \int_v^\infty J_0^2(k_0\beta a) k_0^2 \beta I^{zz}_{Hmn}(\beta) d\beta \end{aligned} \tag{2.42}$$

The third term in the above expression can be evaluated in closed form. This term shall be called Z^{zz}_{Hmn}:

$$Z^{zz}_{Hmn} = 2\pi \int_v^\infty J_0^2(k_0\beta a) k_0^2 \beta I^{zz}_{Hmn}(\beta) d\beta \tag{2.43}$$

For the cases i., ii. and iii. of the previous section an analytical solution will be derived for this infinite β integral.

i. $n = m$

For large beta values one may write:

$$\begin{aligned} k_1 &\approx -jk_0\beta \\ k_2 &\approx -jk_0\beta \\ cosk_1 d &\approx \frac{1}{2} e^{k_0\beta d} \\ sink_1 d &\approx -\frac{j}{2} e^{k_0\beta d} \\ Tm &\approx k_0\beta(\epsilon_r + 1)\left(-\frac{j}{2} e^{k_0\beta d}\right) \end{aligned} \tag{2.44}$$

Substitute these asymptotic forms in $I^{zz}_{mn}(\beta)$ of (2.37). This then gives:

$$I^{zz}_{Hmm} = \frac{j\omega\mu_0}{\epsilon_r} \begin{cases} -\frac{1}{h^2k_0^4\beta^2}\left(\frac{12}{k_0\beta} - 4h\right) - \frac{h\epsilon_r}{3\beta^2k_0^2} & m > 2 \wedge z_{m+1} < d \\ -\frac{1}{h^2k_0^4\beta^2}\left(\frac{10\epsilon_r + 14}{k_0\beta(\epsilon_r+1)} - 4h\right) - \frac{h\epsilon_r}{3\beta^2k_0^2} & m > 2 \wedge z_{m+1} = d \\ -\frac{1}{h^2k_0^4\beta^2}\left(\frac{14}{k_0\beta} - 4h\right) - \frac{h\epsilon_r}{3\beta^2k_0^2} & m = 2 \wedge z_{m+1} < d \\ -\frac{1}{h^2k_0^4\beta^2}\left(\frac{12\epsilon_r + 16}{k_0\beta(\epsilon_r+1)} - 4h\right) - \frac{h\epsilon_r}{3\beta^2k_0^2} & m = 2 \wedge z_{m+1} = d \\ -\frac{1}{h^2k_0^4\beta^2}\left(\frac{6}{k_0\beta} - 2h\right) - \frac{h\epsilon_r}{6\beta^2k_0^2} & m = 1 \wedge z_{m+1} < d \\ -\frac{1}{h^2k_0^4\beta^2}\left(\frac{4\epsilon_r + 8}{k_0\beta(\epsilon_r+1)} - 2h\right) - \frac{h\epsilon_r}{6\beta^2k_0^2} & m = 1 \wedge z_{m+1} = d \end{cases} \tag{2.45}$$

Insert the above expression for $I^{zz}_{Hmn}(\beta)$ in (2.43). Apparently two types of integrals have to be calculated, i.e.

$$\begin{aligned} I_1 &= \int_v^\infty \frac{J_0^2(k_0\beta a)}{\beta} d\beta \\ I_2 &= \int_v^\infty \frac{J_0^2(k_0\beta a)}{\beta^2} d\beta \end{aligned} \tag{2.46}$$

The first integral cannot be calculated analytically, but it can be reduced to a finite integral:

$$\begin{aligned} I_1 &= \int_v^\infty \frac{J_0^2(k_0\beta a)}{\beta} d\beta \\ &= -\log\frac{1}{2}k_0va - \gamma - \int_0^{k_0va} \frac{J_0^2(x) - 1}{x} dx \end{aligned} \tag{2.47}$$

with $\gamma = 0.577215....$ is Euler's constant. The second integral can be evaluated in closed form [5, p. 634]:

$$\begin{aligned} I_2 &= \int_v^\infty \frac{J_0^2(k_0\beta a)}{\beta^2} d\beta \\ &= \frac{J_0^2(k_0va)}{v} - \frac{4k_0a}{\pi} + 2k_0^2a^2v[J_1^2(k_0va) + J_0^2(k_0va)] \\ &\quad -2k_0aJ_0(k_0va)J_1(k_0va) \end{aligned} \tag{2.48}$$

ii. $n = m - 1$

For large beta values $I^{zz}_{mm-1}(\beta)$ of (2.39) takes the form:

$$I^{zz}_{Hmm-1}(\beta) = \frac{j\omega\mu_0}{\epsilon_r}\left\{-\frac{1}{h^2k_0^4\beta^2}\left[2h - \frac{8}{k_0\beta}\right] - \frac{h\epsilon_r}{12\beta^2k_0^2}\right\} \tag{2.49}$$

In order to calculate Z^{zz}_{Hmm-1} we have to use I_1 and I_2 of case i. .

iii. $n \leq m - 2$

Now source term extraction is only used if subdomain m touches subdomain n, thus when n=m-2. For large beta values $I^{zz}_{mn}(\beta)$ of (2.41) reads:

$$I^{zz}_{Hmn}(\beta) = \begin{cases} -\dfrac{2j\omega\mu_0}{\epsilon_r h^2 k_0^5 \beta^3} & n = m-2 \\ 0 & otherwise \end{cases} \tag{2.50}$$

In this case we have to use I_2 of (2.48) in order to find a analytical solution for Z^{zz}_{mn}.

2.6 Efficient evaluation of the excitation vector $[V^z]$

2.6.1 Introduction

In this section the evaluation of the elements of $[V^z]$ will be discussed. Numerical problems involved with the evaluation of the resulting infinite integrals will not be discussed here. An element of $[V^z]$ can be calculated using expression (2.31):

$$V^z_m = -4\pi^2 \int\int_{frill} \vec{\mathcal{H}}_{mwire}(x,y,0).\vec{\mathcal{M}}_{frill}(x,y,0)\; dxdy \tag{2.51}$$

To facilitate the evaluation of the above expression, we shall rewrite it in terms of spectral domain quantities. First divide the magnetic field due to the currents on the wire at the coaxial aperture (z=0) in two components: $\vec{\mathcal{H}}_{mwire} = \mathcal{H}_{mx}\vec{e}_x + \mathcal{H}_{my}\vec{e}_y$. Applying a change to polar coordinates and using (2.4) gives:

$$V^z_m = \frac{4\pi^2 V}{ln(\frac{b}{a})} \int\int_{frill} (\mathcal{H}_{my}\cos\phi - \mathcal{H}_{mx}\sin\phi)\, drd\phi \tag{2.52}$$

with $x = r\cos\phi$ and $y = r\sin\phi$. Both components of the magnetic field at the point (x,y,0) are according to (2.22) given by:

$$\begin{aligned} \mathcal{H}_{mx}(x,y,0) &= \frac{1}{4\pi^2}\int_{-\infty}^{\infty}\int_{-\infty}^{\infty}\int_{z_0} Q_{hxz}(z=0)J_{zm}(z_0)dz_0 e^{-jk_x x}e^{-jk_y y}dk_x dk_y \\ \mathcal{H}_{my}(x,y,0) &= \frac{1}{4\pi^2}\int_{-\infty}^{\infty}\int_{-\infty}^{\infty}\int_{z_0} Q_{hyz}(z=0)J_{zm}(z_0)dz_0 e^{-jk_x x}e^{-jk_y y}dk_x dk_y \end{aligned} \tag{2.53}$$

Substituting (2.53) in (2.52) one obtains:

$$V_m^z = \frac{V}{ln(\frac{b}{a})} \int_{-\infty}^{\infty} \int_{-\infty}^{\infty} \int_{z_0} [Q_{hyz} I_{\phi 1} - Q_{hxz} I_{\phi 2}] J_{zm} dz_0 dk_x dk_y \tag{2.54}$$

with

$$\begin{aligned} I_{\phi 1} &= \int\int_{frill} \cos\phi e^{-jk_x x} e^{-jk_y y} d\phi dr \\ &= \int_a^b \int_0^{2\pi} \cos\phi e^{-jk_0\beta r\cos(\phi-\alpha)} d\phi dr \\ &= \int_a^b \int_0^{2\pi} \cos(\phi'+\alpha) e^{-jk_0\beta r\cos\phi'} d\phi' dr \\ &= \int_a^b \left\{ \int_0^{2\pi} \cos\phi'\cos\alpha e^{-jk_0\beta r\cos\phi'} d\phi' - \int_0^{2\pi} \sin\phi'\sin\alpha e^{-jk\beta r\cos\phi'} d\phi' \right\} dr \\ &= 2\cos\alpha \int_a^b \int_0^{\pi} \cos\phi' e^{-jk_0\beta r\cos\phi'} d\phi' dr \\ &= -2\pi j\cos\alpha \int_a^b J_1(k_0\beta r) dr \\ &= \frac{2\pi j\cos\alpha}{k_0\beta} [J_0(k_0\beta b) - J_0(k_0\beta a)] \end{aligned} \tag{2.55}$$

and

$$\begin{aligned} I_{\phi 2} &= \int\int_{frill} \sin\phi e^{-jk_x x} e^{-jk_y y} d\phi dr \\ &= \frac{2\pi j\sin\alpha}{k_0\beta} [J_0(k_0\beta b) - J_0(k_0\beta a)] \end{aligned} \tag{2.56}$$

In the above derivations use has been made of relations (3.915) and (5.56) of [5]. Because of the radial symmetry of the problem one would expect that the two-dimensional infinite integral of (2.54) can be transformed to a one dimensional integral. This becomes clear if we take a closer look at Q_{hxz} and Q_{hyz} of (2.22):

$$\begin{aligned} Q_{hxz} &= -\frac{jk_0\beta\sin\alpha}{k_1 Tm} [\epsilon_r k_2 \sin k_1(d-z_0) - jk_1\cos k_1(d-z_0)] \quad z=0, z_0>0 \\ Q_{hyz} &= \frac{jk_0\beta\cos\alpha}{k_1 Tm} [\epsilon_r k_2 \sin k_1(d-z_0) - jk_1\cos k_1(d-z_0)] \quad z=0, z_0>0 \end{aligned} \tag{2.57}$$

Use these expressions, (2.55) and (2.56) in order to eliminate one of the two infinite integrals in V_m^z. We then finally obtain:

$$\begin{aligned} V_m^z &= -\frac{4\pi^2 k_0^2 V}{ln(\frac{b}{a})} \int_0^{\infty} \frac{\beta}{k_1 Tm} [J_0(k_0\beta b) - J_0(k_0\beta a)] \\ &\quad \int_{z_0} J_{zm} [\epsilon_r k_2 \sin k_1(d-z_0) - jk_1\cos k_1(d-z_0)] dz_0 d\beta \end{aligned} \tag{2.58}$$

The finite z-integral can be evaluated analytically for the case of rooftop subdomain basis functions. So only one infinite integral remains that has to be calculated numerically. Before a method for the efficient numerical evaluation of this infinite integral is presented, we shall take a closer look to the analytical solution of the z-integral.

2.6.2 Analytical evaluation of the z-integrals

Consider subdomain m according to (2.32). The z_0 integral in V_m^z can now be divided in two parts:

$$V_m^z = -\frac{4\pi^2 k_0^2 V}{ln(\frac{b}{a})} \int_0^\infty \frac{\beta}{k_1 Tm} \left[J_0(k_0\beta b) - J_0(k_0\beta a)\right] J_0(k_0\beta a) I_m^z(\beta) d\beta \tag{2.59}$$

with

$$\begin{aligned} I_m^z(\beta) &= \int_{z_{m-1}}^{z_m} g_m(z_0)[\epsilon_r k_2 \sin k_1(d-z_0) - jk_1 \cos k_1(d-z_0)]dz_0 \\ &+ \int_{z_m}^{z_{m+1}} g_m(z_0)[\epsilon_r k_2 \sin k_1(d-z_0) - jk_1 \cos k_1(d-z_0)]dz_0 \\ &= \frac{2}{k_1^2 h}\{\epsilon_r k_2[2\sin k_1(d-z_m) - \sin k_1(d-z_{m-1}) - \sin k_1(d-z_{m+1})] \\ &\quad -jk_1[2\cos k_1(d-z_m) - \cos k_1(d-z_{m-1}) - \cos k_1(d-z_{m+1})]\} \end{aligned}$$

2.6.3 Improved computational efficiency: source term extraction

The technique to reduce the computation time of the elements of the excitation vector $[V^z]$ is similar to the one discussed in section 2.5.3 for $[Z^{zz}]$. Thus the asymptotic form of the β integrand is extracted for $\beta \geq v$ from the original integrand resulting in a fast converging integral. The infinite integration over this extracted asymptotic form can be done analytically or can be approximated by a closed form expression. Thus:

$$V_m^z = (V_m^z - V_{Hm}^z) + V_{Hm}^z \tag{2.60}$$

with

$$V_{Hm}^z = -\frac{4\pi^2 k_0^2 V}{ln(\frac{b}{a})} \int_v^\infty \frac{\beta}{k_1 Tm} \left[J_0(k_0\beta b) - J_0(k_0\beta a)\right] J_0(k_0\beta a) I_{Hm}^z(\beta) d\beta$$

$\frac{\beta}{k_1 Tm} I_{Hm}^z$ is the asymptotic form of $\frac{\beta}{k_1 Tm} I_m^z$:

$$\frac{\beta}{k_1 Tm} I_{Hm}^z = \begin{cases} \frac{1}{k_0^2\beta} - \frac{2}{k_0^3\beta^2 h} & m = 1 \\ \frac{2}{k_0^3\beta^2 h} & m = 2 \\ 0 & m \geq 3 \end{cases}$$

In order to find a closed form expression for V^s_{Hm} we have to know the following two types of infinite integrals:

$$\begin{aligned} I_1 &= \int_v^\infty \frac{[J_0(k_0\beta b) - J_0(k_0\beta a)]\, J_0(k_0\beta a)}{\beta} d\beta \\ I_2 &= \int_v^\infty \frac{[J_0(k_0\beta b) - J_0(k_0\beta a)]\, J_0(k_0\beta a)}{\beta^2} d\beta \end{aligned} \tag{2.61}$$

Both types of infinite integrals cannot be evaluated analytically, but it is possible to rewrite them in terms of a finite fast converging integral. The first integral I_1 can be divided in two parts:

$$\begin{aligned} I_1 &= \int_v^\infty \frac{J_0(k_0\beta b) J_0(k_0\beta a)}{\beta} d\beta - \int_v^\infty \frac{J_0^2(k_0\beta a)}{\beta} d\beta \\ &= I_{1a} + I_{1b} \end{aligned} \tag{2.62}$$

I_{1b} has already been discussed in the previous paragraph and is given by equation (2.47). The other part of the integral I_{1a} is more difficult to determine. However, if we substitute for the Bessel functions their asymptotic form, a closed form expression for I_{1a} can be found. Let

$$J_0(x) \approx \sqrt{\frac{2}{\pi x}} \left(\cos\left(x - \frac{\pi}{4}\right) + \frac{\sin\left(x - \frac{\pi}{4}\right)}{8x} \right)$$

Using only the first term of this approximation, I_{1a} takes the form:

$$\begin{aligned} I_{1a} &= \int_v^\infty \frac{J_0(k_0\beta b) J_0(k_0\beta a)}{\beta} d\beta \\ &= \int_v^\infty \frac{2}{\pi k_0 \sqrt{ba}} \frac{\cos\left(k_0\beta b - \frac{\pi}{4}\right) \cos\left(k_0\beta a - \frac{\pi}{4}\right)}{\beta^2} d\beta \\ &= \frac{1}{\pi\sqrt{ba}} \left((b+a) \left[\frac{\sin k_0 v(b+a)}{k_0 v(b+a)} - ci(k_0 v(b+a)) \right] \right. \\ &\quad \left. + (b-a) \left[\frac{\cos k_0 v(b-a)}{k_0 v(b-a)} + si(k_0 v(b-a)) \right] \right) \end{aligned} \tag{2.63}$$

$ci(x)$ and $si(x)$ are the cosine resp. sine integral defined by:

$$\begin{aligned} ci(x) &= -\int_x^\infty \frac{\cos t}{t} dt \\ si(x) &= -\int_x^\infty \frac{\sin t}{t} dt \end{aligned}$$

A more accurate result can be obtained if more terms of the asymptotic expansion for J_0 are used. The last step is now to calculate the second type of integral, i.e. I_2. Again this integral will be divided in two parts:

$$\begin{aligned} I_2 &= \int_v^\infty \frac{J_0(k_0\beta b)J_0(k_0\beta a)}{\beta^2}d\beta - \int_v^\infty \frac{J_0^2(k_0\beta a)}{\beta^2}d\beta \\ &= I_{2a} + I_{2b} \end{aligned} \tag{2.64}$$

I_{2b} is given by (2.48). The other part I_{2a} can be expressed in terms of hypergeometric functions and a finite fast converging integral. The final expression for I_{2a} becomes:

$$\begin{aligned} I_{2a} &= \frac{1}{v} - k_0 b F(\frac{1}{2}, -\frac{1}{2}; 1; \left(\frac{a}{b}\right)^2) - \frac{k_0 a^2}{2b} F(\frac{1}{2}, \frac{1}{2}; 2; \left(\frac{a}{b}\right)^2) \\ &\quad - \int_0^v \frac{J_0(k_0\beta b)J_0(k_0\beta a) - 1}{\beta^2}d\beta \end{aligned} \tag{2.65}$$

$F(\alpha, \beta; \gamma; z)$ is a hypergeometric function defined on page 1039 of reference [5].

2.7 Some results

The theory described in the previous sections has been implemented in a FORTRAN computer program. With this program it is possible to determine the unknown current distribution on the wire. Once this current distribution is known the input impedance (see (2.3)) and the radiation characteristics (see chapter 4) can be determined. In this section an example of a wire antenna embedded in a substrate above a groundplane is discussed. The antenna dimensions (see figure 2.1) are given below. This antenna has also been analyzed in [6].

- $z_F = 12mm$
- $d = 12.5mm$
- $\epsilon_r = 2.1 \quad \tan\delta = 0.0005$
- $a = 0.625mm$
- $b = 2.05mm$
- Number of basis functions on wire: $N_z = 5$

From literature of wire antennas in free space it is known that about 20 basis functions per wavelength have to be used in order to obtain acceptable results. Therefore we used 5 basis functions on the wire in this case. Using more basis functions didn't change the results significantly. On the following pages the current distribution, the input impedance and radiation characteristics of the wire antenna are shown. The agreement between our results and results from literature is very good.

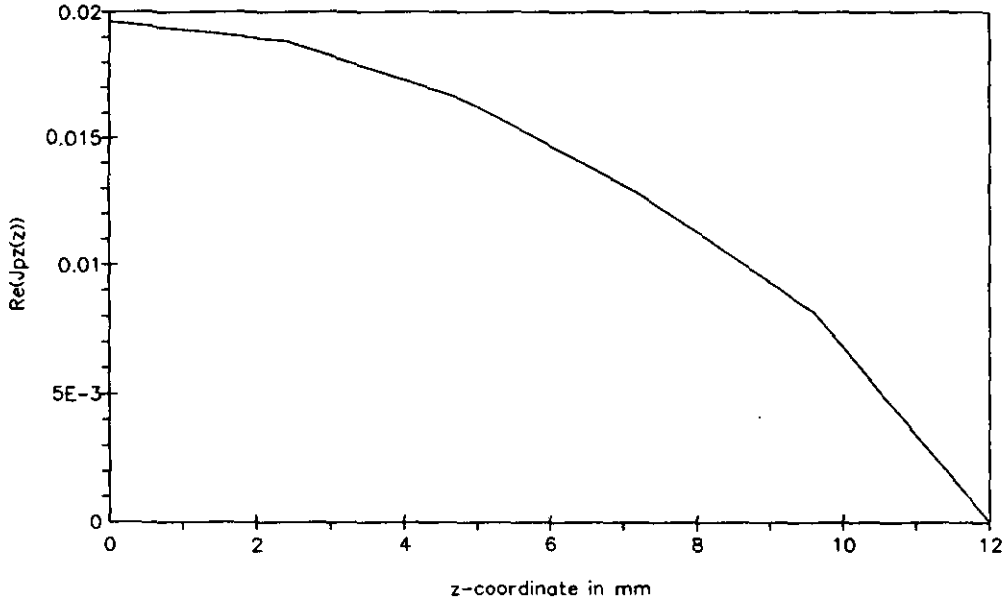

Figure 2.4: Real part of current distribution, f=3.5 GHz

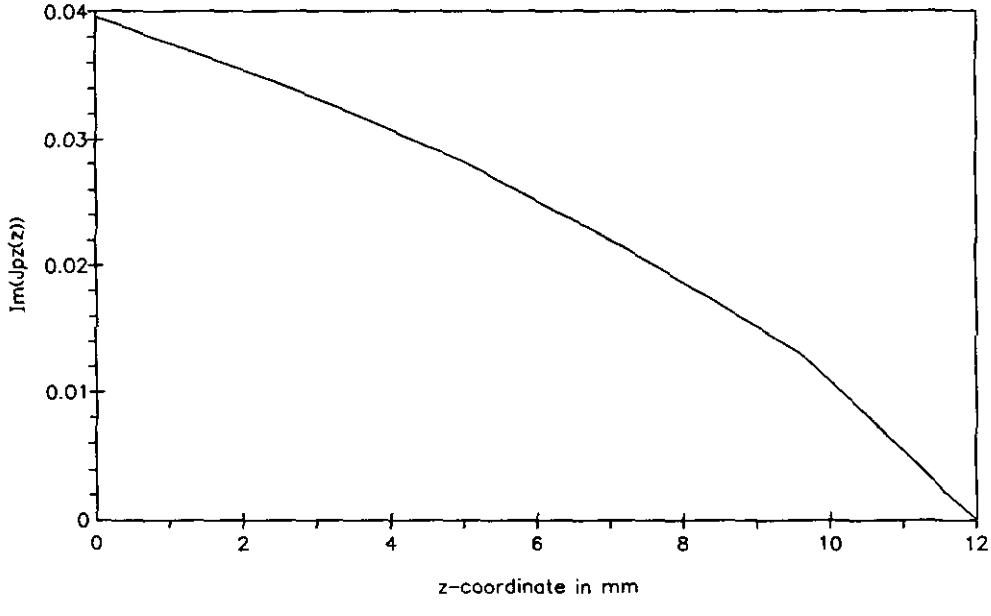

Figure 2.5: Imaginary part of current distribution, f=3.5 GHz

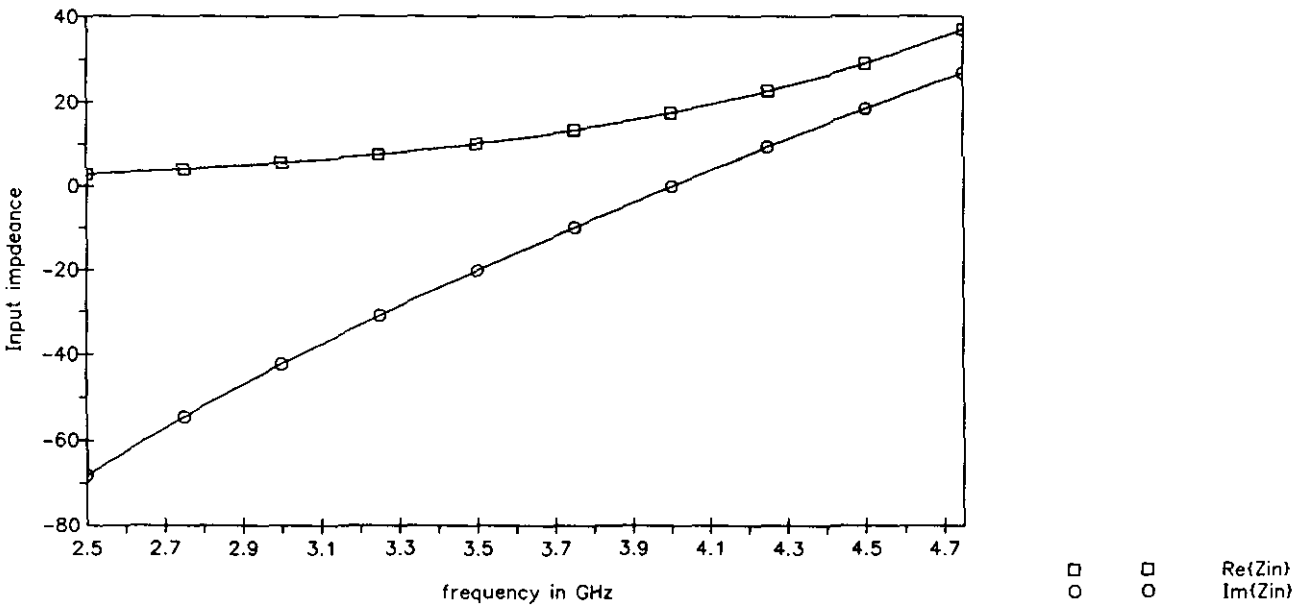

Figure 2.6: Real and imaginary part of input impedance

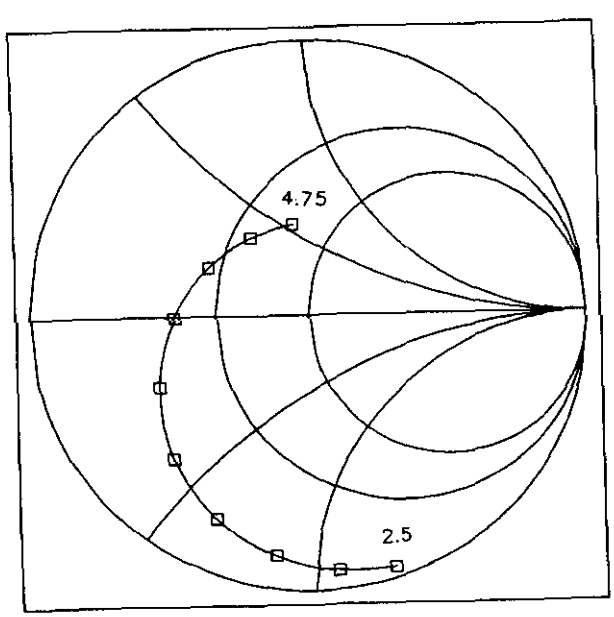

Figure 2.7: Input impedance presented in a Smith chart

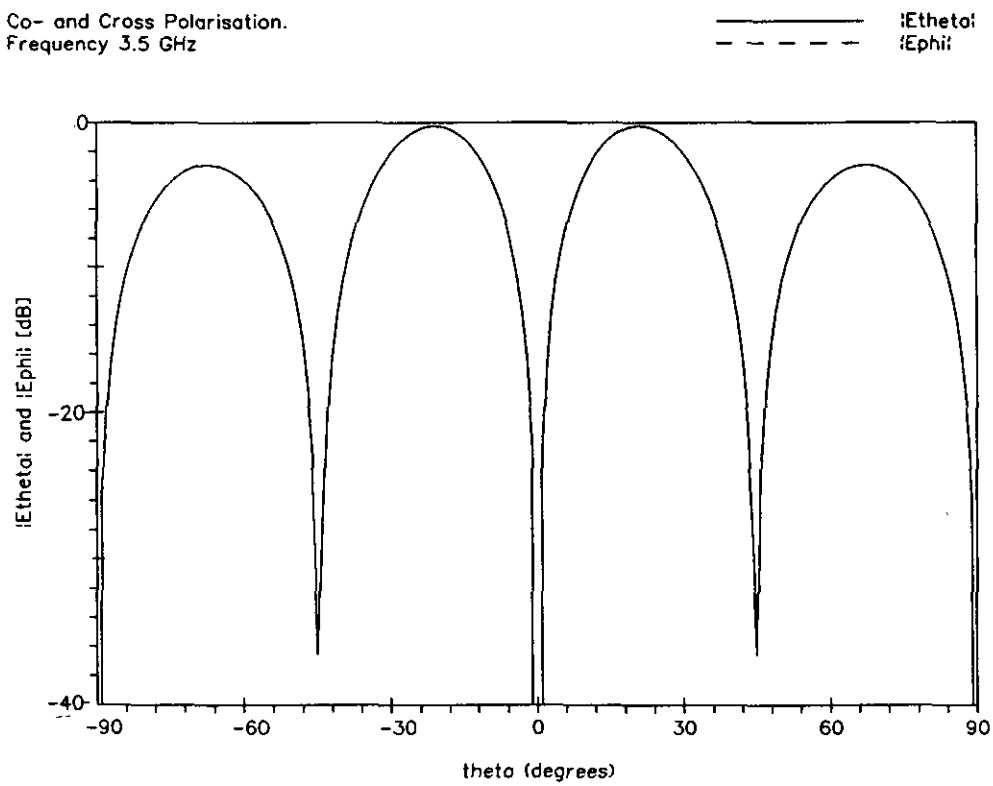

Figure 2.8: Radiation pattern

Chapter 3

Rigorous analysis of thick (broadband) microstrip antennas using a spectral domain moment method

3.1 Introduction

In [1],[4],[7],[8] a model was presented for the analysis of thin substrate microstrip antennas using a so called spectral domain moment method. This model fails if we want to analyse thick microstrip antennas, because the effects of the feeding coaxial probe are not included in the model. Here a more sophisticated and rigorous model of the feeding coaxial structure is presented. Furthermore, a special attachment mode is used to describe the current distribution at the coax-patch transition. A great disadvantage of such a rigorous model is the fact that the computing time becomes very large. However, using the efficiency improvement method described in chapter 2 and in [4] it is possible to obtain accurate results with a minimum of computation time. It should be noted that the method presented here can also be used for the analyses of thin microstrip antennas. Due to the rigorous modelling of the feed and due to the incorporation of an attachment mode in the analyses, the results obtained with this new method for thin microstrip antennas are better than those obtained with the old model of [1],[4],[7],[8].

3.2 Model description

The general structure that we want to analyse is shown in figure 3.1. The patch is located in the $z = z'$ plane and can have a dielectric cover. The feeding coaxial probe, located at (x_s, y_s), may be connected to the patch, but this is not necessary, thus $z_F \leq z'$. The substrate with a complex permittivity ϵ_r and thickness d is located above a perfectly conducting infinite groundplane. We will only consider rectangular microstrip antennas. Extension of this model to other patch shapes is straightforward. The fields of the TEM-mode in the coaxial aperture will be used as a source.

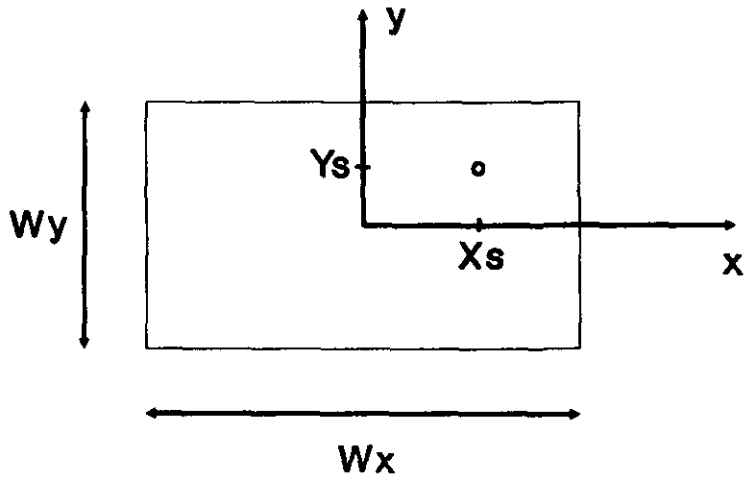

Top View

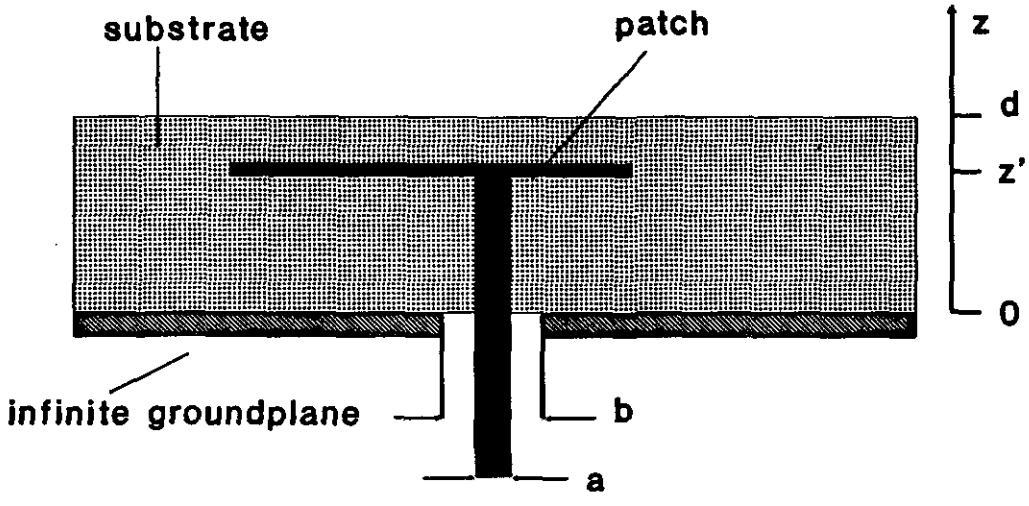

Side View

Figure 3.1: Probe-fed rectangular microstrip antenna

3.3 Moment method formulation for thick microstrip antennas

The moment method formulation is in this case similar to the formulation for the case of a wire antenna (see chapter 2). The only complication is the fact that apart from $\hat{z}$-directed currents we now have $\hat{x}$- and $\hat{y}$-directed currents as well.

3.3.1 Green's function

In [1] the Green's function of a horizontal $\hat{x}$- or $\hat{y}$-directed electric dipole embedded in a substrate above an infinite groundplane are given. In chapter 2 of this report the Green's function for a $\hat{z}$-directed electric dipole was calculated. Combining these two results, the electric field in the substrate in the point (x,y,z) due to a general current distribution in the substrate is given by:

$$\begin{aligned}\vec{\mathcal{E}}_1(x,y,z) &= \frac{1}{4\pi^2}\int_{-\infty}^{\infty}\int_{-\infty}^{\infty}\vec{E}(k_x,k_y,z)e^{-jk_x x}e^{-jk_y y}dk_x dk_y \\ &= \frac{1}{4\pi^2}\int_{-\infty}^{\infty}\int_{-\infty}^{\infty}\int_{z_0}\bar{\bar{Q}}(k_x,k_y,z_0,z).\vec{J}(k_x,k_y,z_0)dz_0 e^{-jk_x x}e^{-jk_y y}dk_x dk_y\end{aligned}$$

With:

$$\bar{\bar{Q}}(k_x,k_y,z_0,z) = \begin{pmatrix} Q_{xx} & Q_{xy} & Q_{xz} \\ Q_{yx} & Q_{yy} & Q_{yz} \\ Q_{zx} & Q_{zy} & Q_{zz} \end{pmatrix} \tag{3.1}$$

$$\begin{aligned}
Q_{xx}(\beta,\alpha,z_0,z) &= \tfrac{\omega\mu_0\sin k_1 z}{\epsilon_r k_1 TeTm}\left[j(\beta^2\cos^2\alpha-\epsilon_r)NeTm-\beta^2\cos^2\alpha k_1^2(\epsilon_r-1)\sin k_1 z_0\right] \\
Q_{xy}(\beta,\alpha,z_0,z) &= Q_{yx} = \tfrac{\omega\mu_0\beta^2\sin k_1 z}{2\epsilon_r k_1 TeTm}\left[jNeTm-k_1^2(\epsilon_r-1)\sin k_1 z_0\right]\sin 2\alpha \\
Q_{xz}(\beta,\alpha,z_0\le z,z) &= -Q_{zx} = \tfrac{\omega\mu_0\beta\cos\alpha\cos k_1 z_0}{k_0\epsilon_r Tm}\left[\epsilon_r k_2\cos k_1(d-z)+jk_1\sin k_1(d-z)\right] \\
Q_{yy}(\beta,\alpha,z_0,z) &= \tfrac{\omega\mu_0\sin k_1 z}{\epsilon_r k_1 TeTm}\left[j(\beta^2\sin^2\alpha-\epsilon_r)NeTm-\beta^2\sin^2\alpha k_1^2(\epsilon_r-1)\sin k_1 z_0\right] \\
Q_{yz}(\beta,\alpha,z_0\le z,z) &= -Q_{zy} = \tfrac{\omega\mu_0\beta\sin\alpha\cos k_1 z_0}{k_0\epsilon_r Tm}\left[\epsilon_r k_2\cos k_1(d-z)+jk_1\sin k_1(d-z)\right] \\
Q_{zz}(\beta,\alpha,z_0,z) &= \tfrac{j\omega\mu_0}{\epsilon_r k_0^2}\delta(z-z_0) \\
&\quad -\tfrac{j\omega\mu_0\beta^2}{\epsilon_r k_1 Tm}\begin{cases}\cos k_1 z_0\left[\epsilon_r k_2\sin k_1(d-z)-jk_1\cos k_1(d-z)\right] & z_0\le z \\ \cos k_1 z\left[\epsilon_r k_2\sin k_1(d-z_0)-jk_1\cos k_1(d-z_0)\right] & z_0\ge z\end{cases}
\end{aligned}$$

and

$$Ne = k_1 \cos k_1(d - z_0) + jk_2 \sin k_1(d - z_0)$$

$$Tm = k_2\epsilon_r \cos k_1 d + jk_1 \sin k_1 d$$

$$Te = k_1 \cos k_1 d + jk_2 \sin k_1 d$$

$$k_1^2 = \epsilon_r k_0^2 - k_x^2 - k_y^2 \qquad (Im(k_1) < 0)$$

$$k_2^2 = k_0^2 - k_x^2 - k_y^2 \qquad (Im(k_2) < 0)$$

$$k_x = k_0\beta\cos\alpha \quad k_y = k_0\beta\sin\alpha$$

The corresponding magnetic field at (x,y,0) is given by:

$$\begin{aligned}\vec{\mathcal{H}}_1(x,y,0) &= \frac{1}{4\pi^2}\int_{-\infty}^{\infty}\int_{-\infty}^{\infty}\vec{H}(k_x,k_y,0)e^{-jk_x x}e^{-jk_y y}dk_x dk_y \\ &= \frac{1}{4\pi^2}\int_{-\infty}^{\infty}\int_{-\infty}^{\infty}\int_{z_0}\bar{\bar{Q}}_h(k_x,k_y,z_0,0).\vec{J}(k_x,k_y,z_0)dz_0 e^{-jk_x x}e^{-jk_y y}dk_x dk_y\end{aligned}$$

With:

$$\bar{\bar{Q}}_h(k_x,k_y,z_0,0) = \begin{pmatrix} Q_{hxx} & Q_{hxy} & Q_{hxz} \\ Q_{hyx} & Q_{hyy} & Q_{hyz} \\ Q_{hzx} & Q_{hzy} & Q_{hzz} \end{pmatrix} \tag{3.2}$$

$$\begin{aligned}
Q_{hxx}(\beta,\alpha,z_0,0) &= \frac{jk_0^2\beta^2(\epsilon_r-1)\sin 2\alpha \sin k_1 z_0}{2TeTm} \\
Q_{hxy}(\beta,\alpha,z_0,0) &= -\frac{Ne}{Te} + \frac{jk_0^2\beta^2(\epsilon_r-1)\sin^2\alpha \sin k_1 z_0}{TeTm} \\
Q_{hxz}(\beta,\alpha,z_0,0) &= -\frac{jk_0\beta\sin\alpha}{k_1 Tm}[\epsilon_r k_2 \sin k_1(d-z_0) - jk_1\cos k_1(d-z_0)] \\
Q_{hyx}(\beta,\alpha,z_0,0) &= \frac{Ne}{Te} - \frac{jk_0^2\beta^2(\epsilon_r-1)\cos^2\alpha \sin k_1 z_0}{TeTm} \\
Q_{hyy}(\beta,\alpha,z_0,0) &= -\frac{jk_0^2\beta^2(\epsilon_r-1)\sin 2\alpha \sin k_1 z_0}{2TeTm} \\
Q_{hyz}(\beta,\alpha,z_0,0) &= \frac{jk_0\beta\cos\alpha}{k_1 Tm}[\epsilon_r k_2 \sin k_1(d-z_0) - jk_1\cos k_1(d-z_0)] \\
Q_{hzx}(\beta,\alpha,z_0,0) &= 0 \\
Q_{hzy}(\beta,\alpha,z_0,0) &= 0 \\
Q_{hzz}(\beta,\alpha,z_0,0) &= 0
\end{aligned}$$

Note that we are only interested in the tangential magnetic field at the coaxial aperture (z=0 plane). Therefore only the case z=0 is considered. The zeros of the functions Te and

Tm correspond to solutions of the characteristic equation for TE respectivily TM surface waves in a dielectric layer on an infinite groundplane. These zeros correspond to poles in the Green's functions. The numerical problems due to these poles will not be discussed in this report. More details can be found in [1, chapter 3].

3.3.2 Matrix equation

A linear matrix equation can be derived by applying the method of moments on the boundary conditions on all the metallic structures . Again we shall use a Galerkin type of solution, i.e. test- and expansion functions are identical. Following the strategy of section 2.4.1, a matrix equation can be derived with the general form:

$$[Z][I] + [V] = [0] \tag{3.3}$$

The vector [I] contains the unknown mode coefficients of the basis functions. The only difference with section 2.4.1 is the fact that we now not only have $\hat{z}$-directed basis functions on the probe, but also $\hat{x}$- and $\hat{y}$-directed basis functions on the patch. The matrix [Z], the excitation vector [V] and the vector [I] can therefore be written in the form:

$$[Z] = \begin{pmatrix} [Z^{aa}] & [Z^{af}] & [Z^{ap}] \\ [Z^{fa}] & [Z^{ff}] & [Z^{fp}] \\ [Z^{pa}] & [Z^{pf}] & [Z^{pp}] \end{pmatrix} \tag{3.4}$$

$$[V] = \begin{pmatrix} [V^a] \\ [V^f] \\ [V^p] \end{pmatrix}$$

$$[I] = \begin{pmatrix} [I^a] \\ [I^f] \\ [I^p] \end{pmatrix}$$

with

$$Z_{mn}^{\alpha\beta} = 4\pi^2 \int\int\int \vec{\mathcal{E}}_n^{\beta}(x,y,z).\vec{\mathcal{J}}_m^{\alpha}(x,y,z)dxdydz$$

$$V_m^{\alpha} = 4\pi^2 \int\int\int \vec{\mathcal{E}}_{source}(x,y,z).\vec{\mathcal{J}}_m^{\alpha}(x,y,z)dxdydz$$

In the above expressions a represents the attachment mode, f the modi on the coaxial feed and p the modi on the patch. Let's assume that there is 1 attachment mode, Nz basis

functions on the feeding probe, Nx $\hat{x}$-directed and Ny $\hat{y}$-directed basis functions on the patch. Then $[Z^{aa}]$ is a 1x1 matrix, $[Z^{fa}]$ a Nz x 1 matrix, $[Z^{pa}]$ a (Nx+Ny) x 1 matrix, $[Z^{pf}]$ a (Nx+Ny) x Nz matrix, $[Z^{ff}]$ a Nz x Nz matrix and $[Z^{pp}]$ a (Nx+Ny) x (Nx+Ny) matrix. Note that due to reciprocity the matrix [Z] is symmetric. In section 3.7 and 3.8 it is discussed how the elements of the 9 submatrices of [Z] and of the excitation vector [V] can be determined in an accurate yet efficient way. Once [Z] and [V] are known, the unknown mode coefficients, [I], can be calculated by solving the matrix equation (3.3). The time needed to solve this equation can usually be neglected compared to the time needed to determine [Z] and [V]. Therefore we have focussed our attention on the efficient calculation of the elements of [Z] and [V].
If the currents on patch and probe are known, the input impedance and radiation pattern can be determined. Let I(z=0) be the total current at the base of the feeding probe. Then the input impedance is given by (see also section 2.2):

$$Z_{in} = \frac{V}{I(z=0)} \tag{3.5}$$

V is the voltage between inner and outer conductor of the coaxial cable. The calculation of the radiation pattern is described in chapter 4 of this report.

3.4 Attachment mode at the patch-coax transition

One of the shortcomings of the thin substrate model of [1],[4],[7],[8] is the fact that the current distribution at the transition between the feeding probe and the patch is not included. This implies that current continuity is not satisfied in this region. To ensure continuity of current along this probe-patch transition a special attachment mode is introduced. Several attachment modes from literature have been considered. The attachment mode introduced in [10] is very rigorous but is very inefficient to use, because it's an infinite summation of cavity modes. The attachment mode used by [9] is computationally efficient but not rigorous, because the dependence of the patch current on the radial distance from the patch-probe transition is described with piece-wise linear and piece-wise constant functions. The attachment mode introduced in this report has an exact $\frac{1}{r}$ dependence yet is computationally very efficient. In figure 3.2 two possible candidates are shown. The outer radius b_a of the attachment mode has to be chosen properly. Tests in literature [11] show that excellent results can be obtained if $0.1\lambda \leq b_a \leq 0.2\lambda$ where λ is the wavelength in the medium of interest.
In formule form these two attachment modes are given by:

$$\begin{aligned} \vec{J}_1^a &= \vec{J}_{1p}^a + \vec{J}_F^a \\ \vec{J}_2^a &= \vec{J}_{2p}^a + \vec{J}_F^a \end{aligned} \tag{3.6}$$

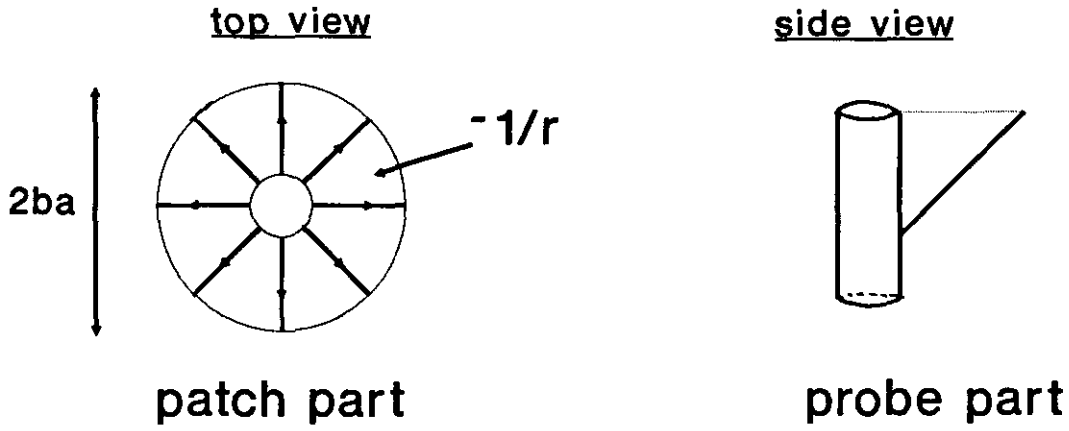

Figure 3.2: Attachmode mode at the patch-probe transition

$\vec{\mathcal{J}}^a_{1p}$ and $\vec{\mathcal{J}}^a_{2p}$ are the patch parts of the two modes:

$$\vec{\mathcal{J}}^a_{1p} = \begin{cases} -\dfrac{r}{2\pi b_a^2}\vec{e}_r & 0 \le r \le a \\ \left(-\dfrac{r}{2\pi b_a^2} + \dfrac{1}{2\pi r}\right)\vec{e}_r & a \le r \le b_a \\ 0 & r \ge b_a \end{cases}$$

$$\vec{\mathcal{J}}^a_{2p} = \begin{cases} \dfrac{b_a^2 - r^2}{2\pi r(b_a^2 - a^2)}\vec{e}_r & a \le r \le b_a \\ 0 & \textit{elsewhere} \end{cases}$$

With $x = r\cos\phi$ and $y = r\sin\phi$. The feed part is in both cases a half rooftop function:

$$\vec{\mathcal{J}}^a_F = \vec{e}_z \frac{1}{2\pi a}\delta\left(\sqrt{(x-x_s)^2 + (y-y_s)^2 - a^2}\right)\frac{2}{h}(z - z' + \frac{h}{2}) \quad z' - \tfrac{h}{2} \le z \le z'$$

We have chosen these two types of possible attachment modes for two reasons. First of all because they ensure continuity of current at the patch-coax transition and second because the Fourier transforms of these two modes is known in closed form. So they can be used

in combination with the spectral domain moment method. Using definition (2.12) for the Fourier transformation, the transforms of the two modes become:

$$\begin{aligned}\vec{J}_1^a(k_x,k_y,z) &= \vec{J}_{1p}^a(k_x,k_y,z) + \vec{J}_f^a(k_x,k_y,z)\\ \vec{J}_2^a(k_x,k_y,z) &= \vec{J}_{2p}^a(k_x,k_y,z) + \vec{J}_f^a(k_x,k_y,z)\end{aligned} \tag{3.7}$$

With

$$\vec{J}_{1p}^a = [\vec{e}_x\cos\alpha + \vec{e}_y\sin\alpha]e^{jk_{x_s}x_s}e^{jk_{y_s}y_s}\left\{\frac{-2jJ_1(k_0\beta b_a)}{b_a k_0^2\beta^2} + \frac{jJ_0(k_0\beta a)}{k_0\beta}\right\}$$

$$\begin{aligned}\vec{J}_{2p}^a &= [\vec{e}_x\cos\alpha + \vec{e}_y\sin\alpha]e^{jk_{x_s}x_s}e^{jk_{y_s}y_s}\left\{\frac{j}{k_0\beta(b_a^2-a^2)}\right\}\\ &\quad\left\{J_0(k_0\beta a)[b_a^2-a^2] + \frac{2aJ_1(k_0\beta a)}{k_0\beta} - \frac{2b_aJ_1(k_0\beta b_a)}{k_0\beta}\right\}\\ \vec{J}_f^a &= \vec{e}_z J_0(k_0\beta a)e^{jk_{x_s}x_s}e^{jk_{y_s}y_s}\frac{2}{h}(z-z'+\frac{h}{2}) \qquad z'-\tfrac{h}{2}\le z\le z'\end{aligned}$$

In the calculation of $\vec{J}_{1p}^a$ and $\vec{J}_{2p}^a$ we have used the property that for a function with a radial dependence of the form $\vec{\mathcal{F}}(r) = \mathcal{F}(r)\vec{e}_r = \mathcal{F}(r)[\vec{e}_x\cos\phi + \vec{e}_y\sin\phi]$, the Fourier transform is given by:

$$\vec{F}(k_x,k_y) = \left[2\pi j\int_0^\infty rJ_1(k_0\beta r)\mathcal{F}(r)dr\right][\vec{e}_x\cos\alpha + \vec{e}_y\sin\alpha] \tag{3.8}$$

In the remaining part of this report only the first type of attachment mode is used. The derivations for the second type are very similar to that of the first one.

3.5 Basis functions on the patch and coaxial probe

Besides the attachment mode the unknown currents on the patch and probe of the microstrip antenna have to be modelled correctly. On the patch entire domain sinusoidal basis functions will be used. The unknown current on the probe is expanded in piece-wise linear (rooftop) basis functions. We have chosen for entire domain basis functions on the patch because only a few of these modes are needed in order to obtain accurate results. If subdomain rooftop basis functions were used on the patch, the number of basis functions would be much larger (often more then 100 [9]). So with subdomain basis functions on the patch it would almost be impossible to analyse finite arrays of microstrip antennas. On the patch the eigenmodes derived with the cavity model [12] are used as a set of basisfunctions.

The basis functions and their Fourier transforms on patch and probe (see section 2.4.2) are given by:

patch

$$\begin{aligned}
\vec{J}^p_{nx}(x,y) = \vec{J}^p_{klx}(x,y) = \quad & \vec{e}_x \frac{1}{W_y} \sin\frac{k\pi}{W_x}(x+\frac{W_x}{2}) \\
& \cos\frac{l\pi}{W_y}(y+\frac{W_y}{2}) \qquad |x| \le \tfrac{W_x}{2}\ |y| \le \tfrac{W_y}{2} \qquad (3.9)\\
\vec{J}^p_{ny}(x,y) = \vec{J}^p_{lky}(x,y) = \quad & \vec{e}_y \frac{1}{W_x} \cos\frac{l\pi}{W_x}(x+\frac{W_x}{2}) \\
& \sin\frac{k\pi}{W_y}(y+\frac{W_y}{2}) \qquad |x| \le \tfrac{W_x}{2}\ |y| \le \tfrac{W_y}{2} \\
& k = 1,2,..\ and\ l = 0,1,2,..
\end{aligned}$$

$$\vec{J}^p_{nx}(k_x,k_y) = \vec{J}^p_{klx}(k_x,k_y) = \vec{e}_x F_s(k,k_x,W_x)F_c(l,k_y,W_y)$$
$$\vec{J}^p_{ny}(k_x,k_y) = \vec{J}^p_{lky}(k_x,k_y) = \vec{e}_y F_c(l,k_x,W_x)F_s(k,k_y,W_y)$$

with

$$F_s(k,k_x,W_x) = \begin{cases} \dfrac{2k\pi W_x \cos\frac{k_x W_x}{2}}{(k\pi)^2-(k_x W_x)^2} & k\ odd \\ \dfrac{-j2k\pi W_x \sin\frac{k_x W_x}{2}}{(k\pi)^2-(k_x W_x)^2} & k\ even \end{cases}$$

$$F_c(l,k_y,W_y) = \begin{cases} \dfrac{-2jW_y k_y \cos\frac{k_y W_y}{2}}{(l\pi)^2-(k_y W_y)^2} & l\ odd \\ \dfrac{-2W_y k_y \sin\frac{k_y W_y}{2}}{(l\pi)^2-(k_y W_y)^2} & l\ even \end{cases}$$

feed

$$\vec{J}^f_{zn}(x,y,z) = \frac{1}{2\pi a}\delta\sqrt{(x-x_s)^2+(y-y_s)^2-a^2}\,g_n(z)\vec{e}_z \qquad (3.10)$$
$$\vec{J}^f_{zn}(k_x,k_y,z) = J_0(k_0\sqrt{k_x^2+k_y^2}a)g_n(z)\vec{e}_z = J_0(k_0\beta a)g_n(z)\vec{e}_z$$

with

$$g_n(z) = \begin{cases} \frac{2}{h}(\frac{h}{2}-z) & n=1 \quad 0 \le z \le \frac{h}{2} \\ \frac{2}{h}(z-z_{n-1}) & n \ge 2 \quad z_{n-1} \le z \le z_n \\ \frac{2}{h}(z_{n+1}-z) & n \ge 2 \quad z_n \le z \le z_{n+1} \end{cases}$$

Note that $z_n = \frac{(n-1)h}{2}$ (see figure 2.3). The first basis function on the probe is a half rooftop function. The mode coefficient of the first basis function is used to determine the input impedance. From convergence tests in literature it is known that using only the (k,l)=(n,0) $\hat{x}$-directed and (l,k)=(0,n) $\hat{y}$-directed entire domain basisfunctions on the patch, accurate results can be obtained. From tests that we have performed we concluded that the results obtained with the model presented in this report don't change significantly by using more basis functions. However, if one uses the model of [1,7,8] without a proper model of the feeding probe, one has to be carefull in choosing an appropriate set of basis functions. In the remaining part of this report the modes with an uniform distribution in the direction perpendicular to the current will be used as a set of basis functions on the patch. Including the other modes is straightforward. The technique to accelerate the method of moments, the so called "source term extraction technique", can also be used for these other modes.

3.6 Source model

The electric field of the TEM mode in the feeding coaxial cable is used as a source exciting the microstrip antenna. This model was also used in chapter 2 for the analyses of wire antennas in a substrate. The magnetic current distribution in the coaxial aperture (z=0 plane) as a function of the applied voltage between inner and outer conductor of the coax is according to (2.4) given by:

$$\vec{\mathcal{M}} = -\frac{V}{r ln(\frac{b}{a})}\vec{e}_\phi \tag{3.11}$$

Once the modecoefficient of the first basis function on the probe is known the input impedance can be determined by using relation (3.5).

3.7 Efficient calculation of the matrix [Z]

The general form of the matrix [Z] is given by equation (3.4). Because of the symmetry of this matrix, only 6 of the 9 submatrices have to be calculated. In this section we shall discuss how the elements of these 6 submatrices can be calculated in an accurate yet computationally efficient way. The numerical problems associated with the evaluation of the resulting infinite integrals will not be discussed in this report. For more details on this topic one is referred to [1],[4]. The asymptotic extraction technique, also called the source term extraction technique, introduced in [4] will be applied here. Using this technique, an element of the matrix [Z] takes the general form after transforming all quantities to the

spectral (k_x, k_y) domain (see (3.4)):

$$\begin{aligned} Z_{mn} &= 4\pi^2 \int\int\int \vec{\mathcal{E}}_n(x,y,z).\vec{\mathcal{J}}_m(x,y,z)dxdydz \\ &= \int_0^\infty \int_{-\pi}^{\pi} \int_z \int_{z_0} [\bar{\bar{Q}}(\beta,\alpha,z_0,z).\vec{J}_n(\beta,\alpha,z_0)]dz_0 \vec{J}_m^*(\beta,\alpha,z)dzk_0^2\beta d\alpha d\beta \\ &= \int_{-\pi}^{\pi}\int_0^\infty f d\beta d\alpha \\ &= \int_{-\pi}^{\pi}\int_0^\infty (f - f_{asymp})d\beta d\alpha + \int_{-\pi}^{\pi}\int_0^\infty f_{asymp} d\beta d\alpha \\ &= (Z_{mn} - Z_{Hmn}) + Z_{Hmn} \end{aligned} \tag{3.12}$$

With $k_x = k_0\beta\cos\alpha$, $k_y = k_0\beta\sin\alpha$ and f_{asymp} is the asymptotic form of the β integrand of Z_{mn} for large β values. In the above formula f_{asymp} is extracted from the original integrand for <u>all</u> β values. In some cases however, we shall extract f_{asymp} from the original integrand for $\beta \geq v$. The infinite β integral of the extracted term Z_{Hmn} can be divided in frequency independent parts. So these elements have to evaluated only once. In the following part of this section the integrand f and it's asymptotic form f_{asymp} will be determined for each of the matrix elements of [Z]. In order to do this the two z-integrations in (3.12) have to be evaluated analytically. Once f and f_{asymp} are known, the extracted terms Z_{Hmn} can also be calculated analytically for most situations.

3.7.1 $[Z^{aa}]$: attachment mode $\longleftrightarrow$ attachment mode

The first type of attachment mode of section 3.4 is now used as an expansion- and as a test function. Because there is only one attachment mode, the submatrix $[Z^{aa}]$ contains only one element. The attachment mode can be divided in two parts, i.e. a patch part and a probe-feed part. Therefore Z^{aa} can be divided in four parts:

$$\begin{aligned} Z^{aa} &= Z_{pp}^{aa} + Z_{pf}^{aa} + Z_{fp}^{aa} + Z_{ff}^{aa} \\ &= Z_{pp}^{aa} + 2Z_{pf}^{aa} + Z_{ff}^{aa} \end{aligned} \tag{3.13}$$

In the above expression p indicates the patch part and f the feed (probe) part of the attachment mode. Again the reciprocity concept can be used to show that $Z_{pf}^{aa} = Z_{fp}^{aa}$. From section 3.4 it is clear that the attachment mode has a radial dependence. Z^{aa} can be written in the form:

$$\begin{aligned} Z^{aa} &= 4\pi^2 \int\int\int \vec{\mathcal{E}}^a(x,y,z).\vec{\mathcal{J}}^a(x,y,z)dxdydz \\ &= \int_0^\infty \int_{-\pi}^{\pi} \int_z \int_{z_0} [\bar{\bar{Q}}(\beta,\alpha,z_0,z).\vec{J}^a(\beta,\alpha,z_0)]dz_0 \vec{J}^{*a}(\beta,\alpha,z)dzk_0^2\beta d\alpha d\beta \end{aligned} \tag{3.14}$$

Fortunately the z integrations and the α integration can be performed in closed form. The remaining infinite β integral has to be evaluated numerically. We shall now examine the three terms of (3.13) in more detail.

i. Z_{pp}^{aa}

The patch part of the attachment mode is z independent. This means that the two z integration can be removed. According to (3.14), (3.7) and (3.1) Z_{pp}^{aa} is given by:

$$\begin{aligned} Z_{pp}^{aa} &= \int_0^{\infty}\int_{-\pi}^{\pi}[\bar{\bar{Q}}(\beta,\alpha,z',z).\vec{J}_p^a(\beta,\alpha)]\vec{J}_p^{*a}(\beta,\alpha)k_0^2\beta d\alpha d\beta \\ &= \int_0^{\infty}\int_{-\pi}^{\pi}\left[Q_{xx}J_{px}^aJ_{px}^{*a}+Q_{xy}J_{py}^aJ_{px}^{*a}+Q_{yx}J_{px}^aJ_{py}^{*a}+Q_{yy}J_{py}^aJ_{py}^{*a}\right]k_0^2\beta d\alpha d\beta \\ &= Z_{pxpx}^{aa}+2Z_{pxpy}^{aa}+Z_{pypy}^{aa} \end{aligned} \quad (3.15)$$

With

$$\begin{aligned} J_{px}^a &= \cos\alpha e^{jk_xx_s}e^{jk_yy_s}\left\{\frac{-2jJ_1(k_0\beta b_a)}{b_ak_0^2\beta^2}+\frac{jJ_0(k_0\beta a)}{k_0\beta}\right\} \\ J_{py}^a &= \sin\alpha e^{jk_xx_s}e^{jk_yy_s}\left\{\frac{-2jJ_1(k_0\beta b_a)}{b_ak_0^2\beta^2}+\frac{jJ_0(k_0\beta a)}{k_0\beta}\right\} \end{aligned}$$

The α integrations of these three double integrals can be calculated in closed form resulting in:

$$\begin{aligned} Z_{pxpx}^{aa}=Z_{pypy}^{aa} &= \pi\int_0^{\infty}\frac{\omega\mu_0\sin k_1z'}{\epsilon_rk_1TeTm}\left[j(\frac{6}{8}\beta^2-\epsilon_r)NeTm\right. \\ &\quad \left.-\frac{6}{8}\beta^2k_1^2(\epsilon_r-1)\sin k_1z'\right]G_{pa}^2k_0^2\beta d\beta \\ Z_{pxpy}^{aa}=Z_{pypx}^{aa} &= \frac{\pi}{2}\int_0^{\infty}\frac{\omega\mu_0\beta^2\sin k_1z'}{2\epsilon_rk_1TeTm}[jNeTm \\ &\quad -k_1^2(\epsilon_r-1)\sin k_1z']G_{pa}^2k_0^2\beta d\beta \end{aligned} \quad (3.16)$$

With

$$G_{pa}=\frac{1}{k_0\beta}\left[\frac{2J_1(k_0\beta b_a)}{b_ak_0\beta}-J_0(k_0\beta a)\right]$$

Combining the above expressions to an expression for Z_{pp}^{aa} and rewriting it, finally results in:

$$\begin{aligned} Z_{pp}^{aa} &= \frac{2\pi j\omega\mu_0}{\epsilon_r}\int_0^{\infty}\frac{-\beta k_1\sin k_1z'}{Tm} \\ &\quad [k_2\epsilon_r\cos k_1(d-z')+jk_1\sin k_1(d-z')]G_{pa}^2d\beta \end{aligned} \quad (3.17)$$

ii. Z_{pf}^{aa}

One z integration can be eliminated because the patch part of the attachment mode is z independent. Z_{pf}^{aa} is therefore a three dimensional integral given by:

$$\begin{aligned} Z_{pf}^{aa} &= \int_0^\infty \int_{-\pi}^{\pi} \int_{z'-h/2}^{z'} [\bar{\bar{Q}}(\beta,\alpha,z_0,z').\vec{J}_f^a(\beta,\alpha,z_0)]dz_0 \vec{J}_p^{*a}(\beta,\alpha)k_0^2\beta d\alpha d\beta \\ &= \int_0^\infty \int_{-\pi}^{\pi} \left[\int_{z'-h/2}^{z'} Q_{xz}J_f^a J_{px}^{*a}dz_0 + \int_{z'-h/2}^{z'} Q_{yz}J_f^a J_{py}^{*a}dz_0\right] k_0^2\beta d\alpha d\beta \end{aligned} \tag{3.18}$$

Using the expressions (3.1) and (3.7) the z- and α integration can be performed analytically. The final expression for Z_{pf}^{aa} is then given by:

$$\begin{aligned} Z_{pf}^{aa} &= \frac{4\pi}{h}\int_0^\infty \frac{j\omega\mu_0\beta}{k_0\epsilon_r Tm}[\epsilon_r k_2 \cos k_1(d-z') + jk_1 \sin k_1(d-z')] \\ &\left[\frac{h\sin k_1 z'}{2k_1} + \frac{\cos k_1 z'}{k_1^2} - \frac{\cos k_1(z'-\frac{h}{2})}{k_1^2}\right] J_0(k_0\beta a)G_{pa}k_0^2\beta d\beta \end{aligned} \tag{3.19}$$

iii. Z_{ff}^{aa}

In this case three integrations, i.e. one α integration and two z integrations, have to be (and can be) done in closed form. Using expression (3.7) for the Fourier transform of the feed part of the attachment mode, results in the following four dimensional integral:

$$\begin{aligned} Z_{ff}^{aa} &= \int_0^\infty \int_{-\pi}^{\pi} \int_{z'-h/2}^{z'} \frac{2}{h}\{z-z'+\frac{h}{2}\} \int_{z'-h/2}^{z'} Q_{zz}(\beta,z_0,z) \\ &\frac{2}{h}\{z_0-z'+\frac{h}{2}\}dz_0 dz J_0^2(k_0\beta a)k_0^2\beta d\alpha d\beta \end{aligned} \tag{3.20}$$

Because the integrand is α independent the α integral can be calculated very easily. The derivation of the remaining two z integrations is essentially similar to the calculation of the z integrations in the case of rooftop basis functions on a wire, described in chapter 2. Therefore we shall only give here the final expression for Z_{ff}^{aa}.

$$Z_{ff}^{aa} = 2\pi \int_0^\infty I_{ff}^{aa}(\beta)J_0^2(k_0\beta a)k_0^2\beta d\beta \tag{3.21}$$

With

$$
\begin{aligned}
I_{jj}^{aa}(\beta) = \; & -\frac{j\omega\mu_0 h}{6k_0^2(\beta^2-\epsilon_r)} - \frac{4j\omega\mu_0\beta^2}{\epsilon_r h^2 k_1^3 Tm} \\
& \left\{ \epsilon_r k_2 \left(-\frac{h\cos k_1(d-z')\cos k_1(z'-\frac{h}{2})}{k_1} - \frac{2\sin k_1(d-z')\cos k_1(z'-\frac{h}{2})}{k_1^2} \right.\right. \\
& + \frac{\sin k_1(d-z'+\frac{h}{2})\cos k_1(z'-\frac{h}{2})}{k_1^2} + \frac{h\cos k_1(d-2z')}{2k_1} \\
& \left. + \frac{h^2\cos k_1(d-z')\sin k_1 z'}{4} + \frac{\sin k_1(d-z')\cos k_1 z'}{k_1^2} \right) \\
& -jk_1 \left(\frac{h\sin k_1(d-z')\cos k_1(z'-\frac{h}{2})}{k_1} - \frac{2\cos k_1(d-z')\cos k_1(z'-\frac{h}{2})}{k_1^2} \right. \\
& + \frac{\cos k_1(d-z'+\frac{h}{2})\cos k_1(z'-\frac{h}{2})}{k_1^2} - \frac{h\sin k_1(d-2z')}{2k_1} \\
& \left.\left. - \frac{h^2\sin k_1(d-z')\sin k_1 z'}{4} + \frac{\cos k_1(d-z')\cos k_1 z'}{k_1^2} \right) \right\}
\end{aligned}
$$

In order to be able to use the source term extraction technique given by (3.12), the asymptotic behaviour of the β integrand of an Z^{aa} element has to be determined. For large β values we may write:

$$
\begin{aligned}
& k_1 \approx -jk_0\beta \\
& k_2 \approx -jk_0\beta \\
& \cos k_1 d \approx \frac{1}{2}e^{k_0\beta d} \\
& \sin k_1 d \approx -\frac{j}{2}e^{k_0\beta d} \\
& \cos k_1(d-z') \approx \begin{cases} \frac{1}{2}e^{k_0\beta(d-z')} & z' < d \\ 1 & z' = d \end{cases} \\
& \sin k_1(d-z') \approx \begin{cases} \frac{-j}{2}e^{k_0\beta(d-z')} & z' < d \\ 0 & z' = d \end{cases} \\
& Tm \approx k_0\beta(\epsilon_r+1)\tfrac{-j}{2}e^{k_0\beta d} \\
& Te \approx -jk_0\beta e^{k_0\beta d} \\
& Ne \approx -jk_0\beta e^{k_0\beta(d-z')}
\end{aligned}
\qquad (3.22)
$$

Substitute these asymptotic expressions in (3.15) , (3.19) and (3.21). Combining these asymptotic forms according to (3.13) results in the following form for the extracted part:

$$Z_H^{aa} = \int_v^\infty \int_{-\pi}^{\pi} \int_z \int_{z_0} [\bar{\bar{Q}}_{approx}(\beta,\alpha,z_0,z).\vec{J}^a(\beta,\alpha,z_0)]dz_0\vec{J}^{*a}(\beta,\alpha,z)dz k_0^2\beta d\alpha d\beta$$

$$= \begin{cases} \dfrac{j\omega\mu_0\pi}{k_0} \int_v^\infty \left(\dfrac{4J_1^2(k_0\beta b_a)}{\epsilon_r b_a^2 k_0^2\beta^2} - \dfrac{8J_1(k_0\beta b_a)J_0(k_0\beta a)}{\epsilon_r b_a h k_0^2\beta^2} \right. \\ \qquad \left. + \dfrac{4J_0^2(k_0\beta a)}{\epsilon_r h k_0\beta} - \dfrac{k_0 h J_0^2(k_0\beta a)}{3\beta} - \dfrac{8J_0^2(k_0\beta a)}{\epsilon_r h^2 k_0^2\beta^2} \right) d\beta & z' < d \quad (3.23) \\ \dfrac{j\omega\mu_0\pi}{k_0} \int_v^\infty \left(\dfrac{8J_1^2(k_0\beta b_a)}{(\epsilon_r+1) b_a^2 k_0^2\beta^2} - \dfrac{16J_1(k_0\beta b_a)J_0(k_0\beta a)}{(\epsilon_r+1) b_a h k_0^2\beta^2} \right. \\ \qquad \left. + \dfrac{8J_0^2(k_0\beta a)}{(\epsilon_r+1) h k_0\beta} - \dfrac{k_0 h J_0^2(k_0\beta a)}{3\beta} - \dfrac{(4\epsilon_r+12)J_0^2(k_0\beta a)}{\epsilon_r(\epsilon_r+1) h^2 k_0^2\beta^2} \right) d\beta & z' = d \end{cases}$$

Note that the asymptotic form for the case that $z' < d$ (patch embedded in substrate) and for the case z'=d (patch on top of substrate) are different. In [4] the same effect has been observed for the case of sinusoidal basis functions on the patch. In (3.23) the lower β integration boundary is v instead of 0. The reason for this is that some parts of the asymptotic form of the β integrand diverge for $\beta \to 0$. The above integral contains four types of infinite integrals. These four types can be evaluated analytically or approximated with a closed form expression. The first type of integral can be evaluated very easily for v=0 [5, 6.575]:

$$I_1 = \int_0^\infty \frac{J_1^2(x)}{x^2} dx = \frac{4}{3\pi} \tag{3.24}$$

The second integral cannot be calculated analytically. For large β values however, the Bessel functions can be replaced by their asymptotic form. We shall use only the first term of the asymptotic form here.

$$\begin{aligned} I_2 &= \int_v^\infty \frac{J_1(bx)J_0(ax)}{x^2} dx \\ &= \int_v^\infty \frac{2}{\pi\sqrt{ba}} \frac{\cos(bx-\frac{3\pi}{4})\cos(ax-\frac{\pi}{4})}{x^3} dx \\ &= -\frac{1}{\pi\sqrt{ba}} \left((a+b)^2 \left[\frac{\cos v(a+b)}{2v^2(a+b)^2} - \frac{\sin v(a+b)}{2v(a+b)} + \frac{1}{2} ci(v(a+b)) \right] \right. \\ &\quad \left. + (a-b)^2 \left[\frac{\sin v(a-b)}{2v^2(a-b)^2} + \frac{\cos v(a-b)}{2v(a-b)} + \frac{1}{2} si(v(a-b)) \right] \right) \end{aligned} \tag{3.25}$$

With

$$ci(x) = -\int_x^\infty \frac{\cos t}{t} dt$$

$$si(x) = -\int_x^\infty \frac{\sin t}{t} dt$$

In order to obtain a more accurate result for I_2 more terms of the asymptotic forms of the two Bessel functions have to be used. Closed form expressions using more terms can also be found. The third and fourth type of integral have already been examined in section 2.5.3.

3.7.2 $[Z^{fa}]$: feed modi $\longleftrightarrow$ attachment mode

This matrix has Nz x 1 elements. Because the attachment mode contains a patch and a probe (feed) part, each element of the submatrix $[Z^{fa}]$ is divided in two parts:

$$\begin{aligned} Z_n^{fa} = Z_n^{af} &= \int_0^\infty \int_{-\pi}^{\pi} \int_z \int_{z_0} [\bar{\bar{Q}}(\beta,\alpha,z_0,z).\vec{J}_{zn}^{f}(\beta,\alpha,z_0)]dz_0\vec{J}^{*a}(\beta,\alpha,z)dzk_0^2\beta d\alpha d\beta \\ &= \int_0^\infty \int_{-\pi}^{\pi} \int_{z_0} [\bar{\bar{Q}}(\beta,\alpha,z_0,z').\vec{J}_{zn}^{f}(\beta,\alpha,z_0)]dz_0\vec{J}_p^{*a}(\beta,\alpha)k_0^2\beta d\alpha d\beta \\ &+ \int_0^\infty \int_{-\pi}^{\pi} \int_z \int_{z_0} [\bar{\bar{Q}}(\beta,\alpha,z_0,z).\vec{J}_{zn}^{f}(\beta,\alpha,z_0)]dz_0\vec{J}_f^{*a}(\beta,\alpha,z)dzk_0^2\beta d\alpha d\beta \\ &= Z_n^{fap} + Z_n^{faf} \end{aligned} \tag{3.26}$$

Again the α- and z integrations can be performed analytically. Now let's examine the first term in more detail.

$$\begin{aligned} Z_n^{fap} &= \int_0^\infty \int_{-\pi}^{\pi} \int_{z_0} [\bar{\bar{Q}}(\beta,\alpha,z_0,z).\vec{J}_{zn}^{f}(\beta,\alpha,z_0)]dz_0\vec{J}_p^{*a}(\beta,\alpha)k_0^2\beta d\alpha d\beta \\ &= \int_0^\infty \int_{-\pi}^{\pi} \int_{z_0} [Q_{xz}J_{zn}^{f}J_{px}^{*a} + Q_{yz}J_{zn}^{f}J_{py}^{*a}]dz_0k_0^2\beta d\alpha d\beta \end{aligned} \tag{3.27}$$

Using (3.1), (3.7) and (3.10) and performing the α- and z integrations analytically, one arrives at the following expression for Z_n^{fap}:

$$\begin{aligned} Z_n^{fap} &= 2\pi \int_0^\infty \frac{j\omega\mu_0\beta}{k_0\epsilon_r Tm} \left[\epsilon_r k_2 \cos k_1(d-z') + jk_1 \sin k_1(d-z')\right] G_{pa} \\ &J_0(k_0\beta a)k_0^2\beta \begin{cases} \dfrac{2}{hk_1^2}\left[1-\cos(k_1\dfrac{h}{2})\right]d\beta & n=1 \\ \dfrac{2}{hk_1^2}\left[2\cos k_1 z_n - \cos k_1 z_{n+1} - \cos k_1 z_{n-1}\right]d\beta & n \geq 2 \end{cases} \end{aligned} \tag{3.28}$$

The second term in (3.26), corresponding to the interaction between the feed part of the attachment mode and the n-th basis function on the feeding probe, can be obtained using the same strategy that was used in section 2.5.2. So again the α- and z integrations can be calculated analytically, resulting in:

$$Z_n^{faf} = 2\pi \int_0^\infty I_{ff}^{faf}(\beta)J_0^2(k_0\beta a)k_0^2\beta d\beta \tag{3.29}$$

With for $n \leq Nz-1$

$$I_{ff}^{faf}(\beta) = \frac{-2j\omega\mu_0\beta^2}{\epsilon_r h^2 k_1^4 Tm}\left\{\epsilon_r k_2\left[h\cos k_1(d-z') + \frac{2\sin k_1(d-z')}{k_1} - \frac{2\sin k_1(d-z'+\frac{h}{2})}{k_1}\right]\right.$$
$$\left. +jk_1\left[h\sin k_1(d-z') - \frac{2\cos k_1(d-z')}{k_1} + \frac{2\cos k_1(d-z'+\frac{h}{2})}{k_1}\right]\right\}$$
$$\begin{cases}\left[1-\cos(k_1\frac{h}{2})\right] & n=1\\ \left[2\cos k_1 z_n - \cos k_1 z_{n+1} - \cos k_1 z_{n-1}\right] & 2\leq n\leq Nz-1\end{cases}$$

and for n=Nz (overlap between feed mode n and the attachment mode):

$$\begin{aligned}I_{ff}^{faf}(\beta) &= \frac{j\omega\mu_0}{\epsilon_r}\{-\frac{h\epsilon_r}{12k_0^2(\beta^2-\epsilon_r)} - \frac{2\beta^2}{h^2k_1^5Tm}\\
&[\epsilon_r k_2\,(-2\cos k_1 z'\sin k_1(d-z') - k_1 h\sin k_1 z'\sin k_1(d-z')\\
&+2\cos k_1(z'-h)\sin k_1(d-z'+\frac{h}{2}) - 4\cos k_1(z'-\frac{h}{2})\sin k_1(d-z'+\frac{h}{2})\\
&-k_1 h\cos k_1(z'-h)\cos k_1(d-z') + 2k_1 h\cos k_1(z'-\frac{h}{2})\cos k_1(d-z')\\
&-2\cos k_1(z'-h)\sin k_1(d-z') + 6\cos k_1(z'-\frac{h}{2})\sin k_1(d-z')\Big)\\
&-jk_1\,(-2\cos k_1 z'\cos k_1(d-z') - k_1 h\sin k_1 z'\cos k_1(d-z')\\
&+2\cos k_1(z'-h)\cos k_1(d-z'+\frac{h}{2}) - 4\cos k_1(z'-\frac{h}{2})\cos k_1(d-z'+\frac{h}{2})\\
&+k_1 h\cos k_1(z'-h)\sin k_1(d-z') - 2k_1 h\cos k_1(z'-\frac{h}{2})\sin k_1(d-z')\\
&-2\cos k_1(z'-h)\cos k_1(d-z') + 6\cos k_1(z'-\frac{h}{2})\cos k_1(d-z')\Big)\Big]\ \}\end{aligned}$$

If n=1, i.e. Nz=1 then $z'-h$ and $z'-\frac{h}{2}$ should be set to zero in the above expression for $I_{ff}^{faf}(\beta)$.

Similar to the case of Z^{aa}, we want to use the source term extraction technique to improve the computational efficiency. Using the asymptotic forms of (3.22) an asymptotic form of the β integrand of an element of $[Z^{fa}]$ can be found. We now observe that the asymptotic form of the β integrand is unequal zero only if feed mode n attaches or overlaps the

attachment mode. We then finally get:

$$Z_{Hn}^{fa} = \int_v^\infty \int_{-\pi}^{\pi} \int_z \int_{z_0} [\bar{\bar{Q}}_{approx}(\beta,\alpha,z_0,z).\vec{J}_{zn}^{f}(\beta,\alpha,z_0)]dz_0\vec{J}^{*a}(\beta,\alpha,z)dzk_0^2\beta d\alpha d\beta$$

$$= \frac{2j\omega\mu_0\pi}{\epsilon_r} \begin{cases} \displaystyle\int_v^\infty \frac{-2J_0^2(k_0\beta a)}{h^2k_0^3\beta^2}d\beta & n = Nz-1 \\ \displaystyle\int_v^\infty \left(-\frac{\epsilon_r h J_0^2(k_0\beta a)}{12\beta} + \frac{2J_1(k_0\beta b_a)J_0(k_0\beta a)}{b_a h\beta^2 k_0^3}\right. & \\ \left. + \frac{6J_0^2(k_0\beta a)}{h^2\beta^2k_0^3} - \frac{2J_0^2(k_0\beta a)}{h\beta k_0^2}\right)d\beta & n = Nz \ \wedge \ d < z' \\ \displaystyle\int_v^\infty \left(-\frac{\epsilon_r h J_0^2(k_0\beta a)}{12\beta} + \frac{4\epsilon_r J_1(k_0\beta b_a)J_0(k_0\beta a)}{b_a h\beta^2 k_0^3(\epsilon_r+1)}\right. & \\ \left. + \frac{(4\epsilon_r+8)J_0^2(k_0\beta a)}{h^2\beta^2k_0^3(\epsilon_r+1)} - \frac{2J_0^2(k_0\beta a)}{h\beta k_0^2}\right)d\beta & n = Nz \ \wedge \ d = z' \end{cases} \tag{3.30}$$

The three types of infinite integrals in Z_{Hn}^{fa} can be evaluated in closed form or approximated by a closed form expression. These integrals have already been discussed in the previous section.

3.7.3 $[Z^{pa}]$: patch modi $\longleftrightarrow$ attachment mode

Again divide an element of the submatrix $[Z^{pa}]$ in two parts:

$$\begin{aligned} Z_n^{pa} = Z_n^{ap} &= \int_0^\infty \int_{-\pi}^{\pi} \int_{z_0} [\bar{\bar{Q}}(\beta,\alpha,z_0,z').\vec{J}^{a}(\beta,\alpha,z_0)]dz_0\vec{J}_n^{*p}(\beta,\alpha)k_0^2\beta d\alpha d\beta \\ &= \int_0^\infty \int_{-\pi}^{\pi} [\bar{\bar{Q}}(\beta,\alpha,z',z').\vec{J}_p^{a}(\beta,\alpha)]\vec{J}_n^{p*}(\beta,\alpha)k_0^2\beta d\alpha d\beta \\ &+ \int_0^\infty \int_{-\pi}^{\pi} \int_{z_0} [\bar{\bar{Q}}(\beta,\alpha,z_0,z').\vec{J}_f^{a}(\beta,\alpha,z_0)]dz_0\vec{J}_n^{p*}(\beta,\alpha)k_0^2\beta d\alpha d\beta \\ &= Z_n^{pap} + Z_n^{paf} \end{aligned} \tag{3.31}$$

The sinusoidal basis functions on the rectangular patch do not have a radial symmetry, which implies that the α integration cannot be calculated analytically. The z integration in Z_n^{paf} however, can be performed analytically. So a two dimensional integral over α and β remains that has to be evaluated numerically. Because of the symmetry in the α integrand of Z_n^{pap} and Z_n^{paf} the integration range can be reduced to $0 \rightarrow \frac{\pi}{2}$. We will only consider $\hat{x}$-directed patch basis functions in this section. The derivation for $\hat{y}$-directed basis functions is analogous. Making use of the α symmetry we finally obtain for a $\hat{x}$-directed sinusoidal

patch basis function:

$$\begin{aligned} Z_{nx}^{pap} &= \int_0^\infty \frac{-j\omega\mu_0 k_1 \beta \sin k_1 z'}{\epsilon_r T m} \left(\frac{-2jJ_1(k_0\beta b_a)}{b_a k_0^2 \beta^2} + \frac{jJ_0(k_0\beta a)}{k_0\beta} \right) \\ &\quad (k_2\epsilon_r \cos k_1(d-z') + jk_1 \sin k_1(d-z'))\, I_n^\alpha(\beta) d\beta \\ Z_{nx}^{paf} &= \int_0^\infty \frac{2\omega\mu_0 k_0 \beta^2}{h k_1 \epsilon_r T m} (k_2\epsilon_r \cos k_1(d-z') + jk_1 \sin k_1(d-z')) \\ &\quad \left(\frac{h}{2} \sin k_1 z' + \frac{\cos k_1 z'}{k_1} - \frac{\cos k_1(z'-\frac{h}{2})}{k_1} \right) J_0(k_0\beta a) I_n^\alpha(\beta) d\beta \end{aligned} \tag{3.32}$$

With $I_n^\alpha(\beta)$ given by:

$$I_n^\alpha(\beta) = \begin{cases} 4j \int_0^{\frac{\pi}{2}} \cos\alpha \sin(k_0\beta x_s \cos\alpha) \cos(k_0\beta y_s \sin\alpha) J_{nx}^{*p}(\beta,\alpha) d\alpha & n \text{ odd} \\ 4 \int_0^{\frac{\pi}{2}} \cos\alpha \cos(k_0\beta x_s \cos\alpha) \cos(k_0\beta y_s \sin\alpha) J_{nx}^{*p}(\beta,\alpha) d\alpha & n \text{ even} \end{cases} \tag{3.33}$$

Now let's take a closer look at the asymptotic form of the β integrand of a Z_{nx}^{pa} element in order to be able to use the source term extraction technique. Using (3.22) we find that:

$$\begin{aligned} Z_{Hnx}^{pa} &= \int_v^\infty \int_{-\pi}^{\pi} \int_{z_0} [\bar{\bar{Q}}_{approx}(\beta,\alpha,z_0,z').\vec{J}_a(\beta,\alpha,z_0)] dz_0 \vec{J}_{nx}^{*p}(\beta,\alpha) k_0^2 \beta d\alpha d\beta \\ &= j\omega\mu_0 \int_v^\infty d\beta I_n^\alpha(\beta) \\ &\quad \left(-\frac{jJ_1(k_0\beta b_a)}{k_0 b_a} + \frac{jJ_0(k_0\beta a)}{k_0 h} - \frac{j\epsilon_r J_0(k_0\beta a)}{2\beta} \right) \begin{cases} \frac{1}{\epsilon_r} & z' < d \\ \frac{2}{\epsilon_r + 1} & z' = d \end{cases} \end{aligned} \tag{3.34}$$

Unfortunately we haven't been able to find an analytical solution for the infinite β integral in (3.34).

3.7.4 $[Z^{ff}]$: feed modi $\longleftrightarrow$ feed mode

In chapter 2 of this report an efficient way to calculate the elements of the matrix $[Z^{ff}]$ has already been discussed.

3.7.5 $[Z^{pf}]$: patch modi $\longleftrightarrow$ feed mode

For an arbitrarily basis function $\vec{J}_m^p$ on the patch and $\vec{J}_n^f$ on the feeding probe, an element of the submatrix $[Z^{pf}]$ is given by:

$$Z_{mn}^{pf} = Z_{nm}^{fp} = \int_0^{\infty} \int_{-\pi}^{\pi} \int_{z_0} [\bar{\bar{Q}}(\beta, \alpha, z_0, z').\vec{J}_n^f(\beta, \alpha, z_0)] dz_0 \vec{J}_m^{*p}(\beta, \alpha) k_0^2 \beta d\alpha d\beta \qquad (3.35)$$

The patch is rectangular which implies that the basis functions on the patch have no radial symmetry. Therefore the α-integral in the above expression cannot be eliminated, but can be reduced to the range $0 \longrightarrow \frac{\pi}{2}$ due to the symmetry in the integrand. Fortunately the z-integral can be performed analytically. An element of $[Z^{pf}]$ can be expressed in terms of a two dimensional integral which has to be evaluated numerically. After eliminating the z-integration we finally obtain for a $\hat{x}$-directed patch basis function:

$$\begin{aligned} Z_{mxn}^{pf} &= \int_0^{\infty} \frac{2\omega\mu_0 k_0 \beta^2}{h k_1^2 \epsilon_r T m} (k_2 \epsilon_r \cos k_1(d-z') + j k_1 \sin k_1(d-z')) \\ & J_0(k_0\beta a) I_m^{\alpha}(\beta) \begin{cases} \left[1 - \cos(k_1 \frac{h}{2})\right] d\beta & n = 1 \\ [2\cos k_1 z_n - \cos k_1 z_{n-1} - \cos k_1 z_{n+1}]\, d\beta & n \geq 2 \end{cases} \end{aligned} \qquad (3.36)$$

$I_m^{\alpha}(\beta)$ is defined in (3.33). For $\hat{y}$-directed patch basis functions a similar expression can be derived. The extracted term Z_{Hmn}^{pf} is equal to zero for all basis functions on the feed except if subdomain n touches the patch. So for $\hat{x}$-directed patch basis functions Z_{Hmn}^{pf} is given by:

$$Z_{Hmxn}^{pf} = \begin{cases} 0 & z_{n+1} < z' \\ \frac{\omega\mu_0}{h\epsilon_r k_0} \int_v^{\infty} J_0(k_0\beta a) I_m^{\alpha}(\beta) d\beta & z_{n+1} = z' < d \\ \frac{2\omega\mu_0}{h(\epsilon_r + 1) k_0} \int_v^{\infty} J_0(k_0\beta a) I_m^{\alpha}(\beta) d\beta & z_{n+1} = z' = d \end{cases} \qquad (3.37)$$

An analytical solution for the above infinite integral hasn't been found yet.

3.7.6 $[Z^{pp}]$: patch modi $\longleftrightarrow$ patch mode

An efficient method for the evaluation of the $(Nx + Ny)^2$ elements of the submatrix $[Z^{pp}]$ has already been presented in [4].

3.8 Efficient calculation of the excitation vector [V]

The excitation vector [V] can be divided in three subvectors according to (3.4). the evaluation of each of the elements of these three submatrices will be discussed here. As in the case of the matrix [Z], we will use the extraction technique to improve the efficiency of the method of moments. An element of [V] is given by (see section 2.6):

$$\begin{aligned} V_m &= -4\pi^2 \int\int_{frill} \vec{\mathcal{H}}_m(x,y,0).\vec{\mathcal{M}}_{frill}(x,y,0)\, dxdy \\ &= \frac{4\pi^2 V}{ln(\frac{b}{a})} \int\int_{frill} (\mathcal{H}_{my}\cos\phi - \mathcal{H}_{mx}\sin\phi)\, drd\phi \end{aligned} \tag{3.38}$$

with $x = r\cos\phi$ and $y = r\sin\phi$. $\vec{\mathcal{M}}_{frill}$ is given by (3.11). We shall now take a closer look at the elements of each of the three submatrices of [V].

3.8.1 $[V^a]$: attachment mode

$[V^a]$ contains only one element because there is only one attachment mode. Divide this element in two parts, one related to the patch part of the attachment mode and one related to the probe part of the attachment mode.

$$V^a = V^{af} + V^{ap} \tag{3.39}$$

The derivation of V^{af} is analogous to the derivation of an element of $[V^f]$ which has already been discussed in section 2.6. The result is:

$$V^{af} = -\frac{4\pi^2 k_0^2 V}{ln(\frac{b}{a})} \int_0^\infty \frac{\beta}{k_1 Tm} \left[J_0(k_0\beta b) - J_0(k_0\beta a)\right] J_0(k_0\beta a) I_v^{af}(\beta) d\beta \tag{3.40}$$

with

$$\begin{aligned} I_v^{af}(\beta) &= \frac{2}{k_1^2 h} \Big\{ \epsilon_r k_2 [\frac{hk_1}{2}\cos k_1(d-z') - \sin k_1(d-z'+\frac{h}{2}) + \sin k_1(d-z')] \\ &\quad -jk_1[\frac{-hk_1}{2}\sin k_1(d-z') - \cos k_1(d-z'+\frac{h}{2}) + \cos k_1(d-z')] \Big\} \end{aligned}$$

According to (3.38) the second part, i.e. V^{ap}, is given by:

$$\begin{aligned} V^{ap} &= \frac{4\pi^2 V}{ln(\frac{b}{a})} \int\int_{frill} \left(\mathcal{H}_y^{ap}\cos\phi - \mathcal{H}_x^{ap}\sin\phi\right) dr d\phi \\ &= \frac{V}{ln(\frac{b}{a})} \int\int_{frill} \int_{-\infty}^{\infty}\int_{-\infty}^{\infty} \left\{\left(Q_{hyx}J_{px}^a + Q_{hyy}J_{py}^a\right)\cos\phi \right. \\ &\quad \left. - \left(Q_{hxx}J_{px}^a + Q_{hxy}J_{py}^a\right)\sin\phi\right\} e^{-jk_x x} e^{-jk_y y} dk_x dk_y dr d\phi \\ &= \frac{V}{ln(\frac{b}{a})} \int_{-\infty}^{\infty}\int_{-\infty}^{\infty} e^{-jk_x x_o} e^{-jk_y y_o} \left\{\left(Q_{hyx}J_{px}^a + Q_{hyy}J_{py}^a\right) I_{\phi 1}\right. \\ &\quad \left. - \left(Q_{hxx}J_{px}^a + Q_{hxy}J_{py}^a\right) I_{\phi 2}\right\} dk_x dk_y \\ &= \frac{2j\pi k_0 V}{ln(\frac{b}{a})} \int_0^{\infty}\int_{-\pi}^{\pi} [J_0(k_0\beta b) - J_0(k_0\beta a)] \left\{\frac{-2jJ_1(k_0\beta b_a)}{b_a k_0^2\beta^2} + \frac{jJ_0(k_0\beta a)}{k_0\beta}\right\} \\ &\quad \left(Q_{hyx}\cos^2\alpha + Q_{hyy}\cos\alpha\sin\alpha - Q_{hxx}\cos\alpha\sin\alpha - Q_{hxy}\sin^2\alpha\right) d\alpha d\beta \end{aligned} \tag{3.41}$$

In the above derivation relation (2.55), (2.56) and (3.7) are used. Note that $z = 0$ and $z_0 = z'$. From (3.1) it is clear that the α integration in the above expression can be evaluated analytically. Doing this and rewriting (3.41) then gives:

$$\begin{aligned} V^{ap} &= \frac{4j\pi^2 k_0 V}{ln(\frac{b}{a})} \int_0^{\infty} [J_0(k_0\beta b) - J_0(k_0\beta a)] \left\{\frac{-2jJ_1(k_0\beta b_a)}{b_a k_0^2\beta^2} + \frac{jJ_0(k_0\beta a)}{k_0\beta}\right\} \\ &\quad \frac{1}{Tm}\left(k_2\epsilon_r\cos k_1(d-z') + jk_1\sin k_1(d-z')\right) d\beta \end{aligned} \tag{3.42}$$

The term V_h^a used for the extraction technique

$$V^a = [V^a - V_h^a] + V_h^a$$

is equal to zero in most of the practical situations. Only for the case that the probe part of the attachment mode touches the groundplane (z=0) V_h^a is not equal zero and is given by:

$$V_h^a = \begin{cases} 0 & \frac{h}{2} < z' \\ \dfrac{-4\pi^2 k_0^2 V}{ln(\frac{b}{a})} \displaystyle\int_v^{\infty} \frac{2}{hk_0^3\beta^2} J_0(k_0\beta a)\,[J_0(k_0\beta b) - J_0(k_0\beta a)]\, d\beta & \frac{h}{2} = z' \end{cases} \tag{3.43}$$

A closed form expression for the above infinite integral is given in section 2.6.3 by expression (2.64).

3.8.2 $[V^f]$: feed modi

The determination of these elements has already been discussed in section 2.6 of this report.

3.8.3 $[V^p]$: patch modi

The strategy used in the previous sections can also be applied here. For the m-th $\hat{x}$-directed patch basis function the final expression for V_m^p is given by:

$$V_m^p = \frac{2j\pi k_0 V}{ln(\frac{b}{a})} \int_0^\infty [J_0(k_0\beta b) - J_0(k_0\beta a)] \int_0^{\frac{\pi}{2}} (Q_{hyx}\cos\alpha - Q_{hxx}\sin\alpha)\, J_{mx}^p \cos(k_0\beta y_s \sin\alpha) \begin{cases} -4j\sin(k_0\beta x_s\cos\alpha)d\alpha d\beta & m\ odd \\ 4\cos(k_0\beta x_s\cos\alpha)d\alpha d\beta & m\ even \end{cases} \tag{3.44}$$

With

$$Q_{hyx}\cos\alpha - Q_{hxx}\sin\alpha = \frac{\cos\alpha}{Tm}[k_2\epsilon_r\cos k_1(d-z') + jk_1\sin k_1(d-z')]$$

In the case of $\hat{y}$-directed patch basis functions a similar expression can be derived. Because the patch never touches the groundplane, the extraction technique doesn't have to be used here. The β-integrand converges very fast to zero ($\sim e^{-\beta}$).

3.9 Some applications

The model discussed in the previous sections of this chapter has been implemented in a FORTRAN computer program called EUMAT (Eindhoven University Microstrip antenna Analysis for Thick substrates). With this program it is possible to calculate the input impedance and the radiation characteristics of thick microstrip antennas. The theory for the calculation of the radiation characteristics (far field patterns) is discussed in chapter 4. We have compared our calculations with experiments performed in literature. In most cases a very good agreement has been found, both for thick and thin substrates. Three applications of the software package will be presented here, namely two conventional (electrically) thick microstrip antennas and one electromagnetically coupled thick microstrip antenna. The first antenna is a rectangular microstrip antenna which has been investigated experimentally by Chang [13]. The antenna dimensions are:

- patch location $z' = 3.175mm$
- substrate thickness $d = 3.175mm$
- permittivity $\epsilon_r = 2.33$
- patch dimensions $W_x = 11mm$ $W_y = 17mm$
- inner radius coax $a = 0.635mm$
- outer radius coax $b = 2.1mm$

- excitation point $X_s = 4mm,\ Y_s = 0$

In figure 3.3 and 3.4 the calculated and measured [13] input impedance results are shown. The calculated E-plane and H-plane radiation patterns are given in figure 3.5 and 3.6. The second antenna is also a conventional rectangular microstrip antenna on a (electrically) thick substrate. The antenna dimensions are:

- patch location $z' = 21.6mm$
- substrate thickness $d = 21.6mm$
- permittivity $\epsilon_r = 2.05\ \ \tan\delta = 0.0005$
- patch dimensions $W_x = W_y = 67.9mm$
- inner radius coax $a = 1.5mm$
- outer radius coax $b = 5mm$
- excitation point $X_s = 21.95mm,\ Y_s = 0$

In figure 3.7 and 3.8 the calculated and measured values of the real and imaginary part of the input impedance are shown. The agreement between measurements and calculations is very good. In figure 3.9 and 3.10 the calculated E-plane and H-plane radiation patterns of the antenna are given for f=1.2 GHz. A great disadvantage of thick substrate microstrip antennas is the fact that it is difficult to match these antennas to 50Ω. Because of the inductive shift in the input impedance of this thick substrate microstrip antenna, the use of a compensating network is necessary. The use of such a network would increase the complexity (and production costs) of the total antenna. A possible solution for this problem can be the second antenna that we have investigated. In this case the patch is electromagnetically coupled to the coaxial probe, i.e. $z_F < z'$. The dimensions of this antenna are:

- patch location $z' = 21.8mm$
- substrate thickness $d = 21.8mm$
- probe height $z_F = 21.55mm$
- permittivity $\epsilon_r = 2.05\ \ \tan\delta = 0.0005$
- patch dimensions $W_x = W_y = 38mm$
- inner radius coax $a = 1.5mm$
- outer radius coax $b = 5mm$
- excitation point $X_s = 16mm,\ Y_s = 0$

In figure 3.11 and 3.12 the calculated input impedance and VSWR ratio are shown for this antenna. The bandwidth of the antenna is better than 40 % (VSWR < 2). The calculated E- and H-plane radiation patterns of this antenna are given in figure 3.13 and 3.14 for f=2 GHz. The far field characteristics of this antenna are not so good as the radiation patterns of the previous two antennas. Due to the (long) probe, the patterns are asymmetrical and the cross-polarisation level is higher.

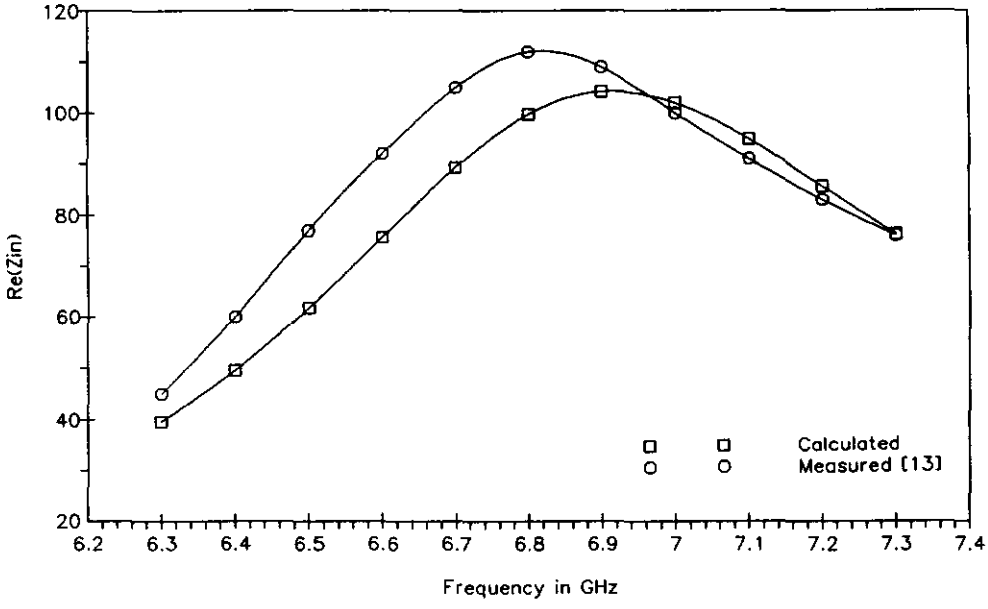

Figure 3.3: Real part of input impedance (measured [13] and calculated)

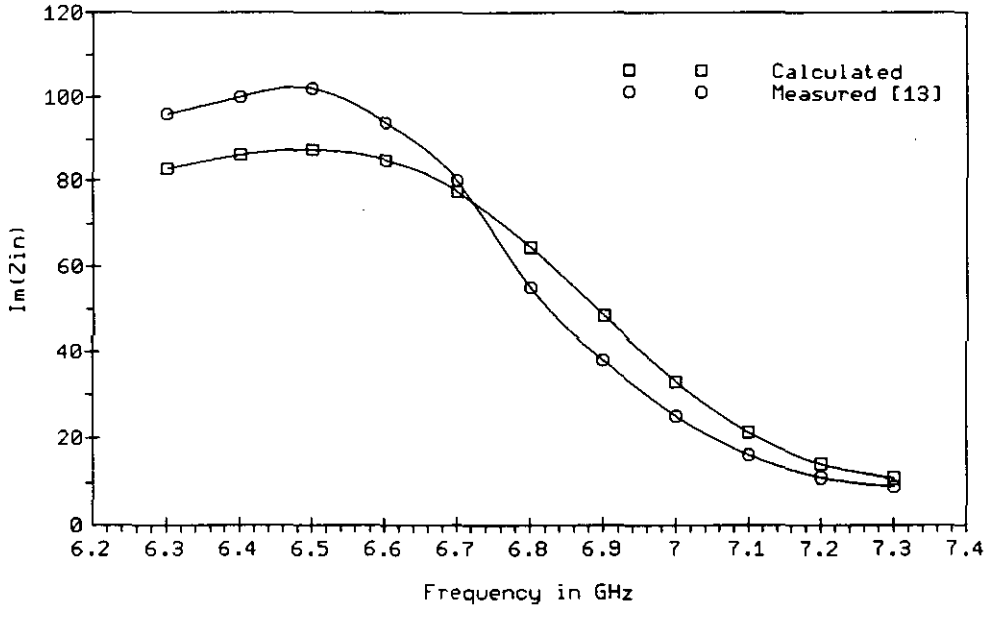

Figure 3.4: Imaginary part of input impedance (measured [13] and calculated)

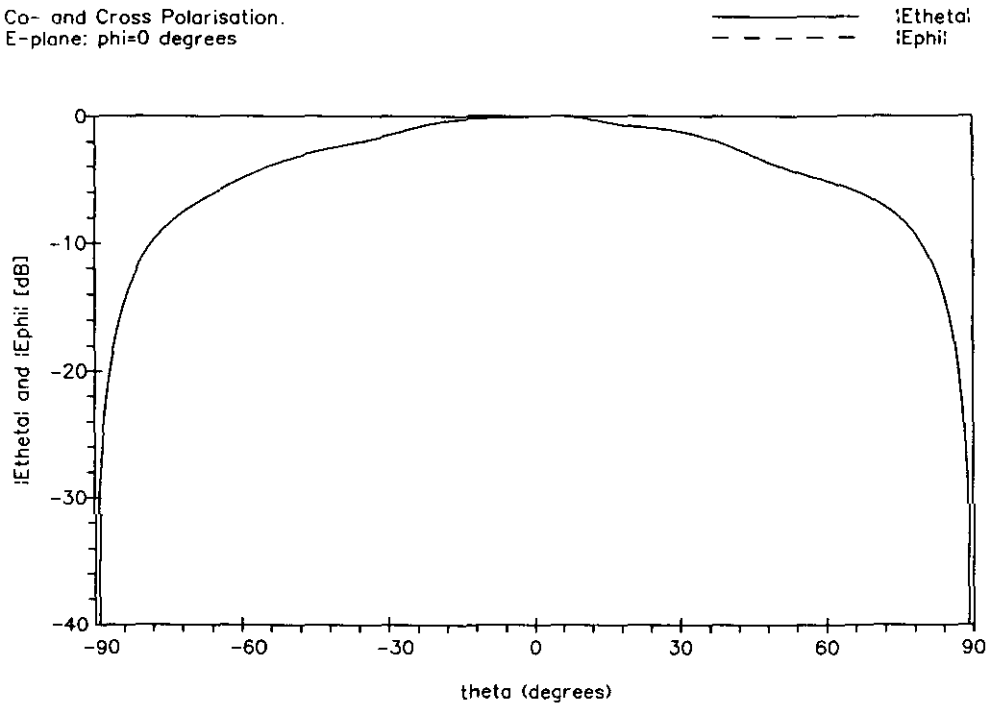

Figure 3.5: Calculated E-plane radiation pattern, f=6.9 GHz

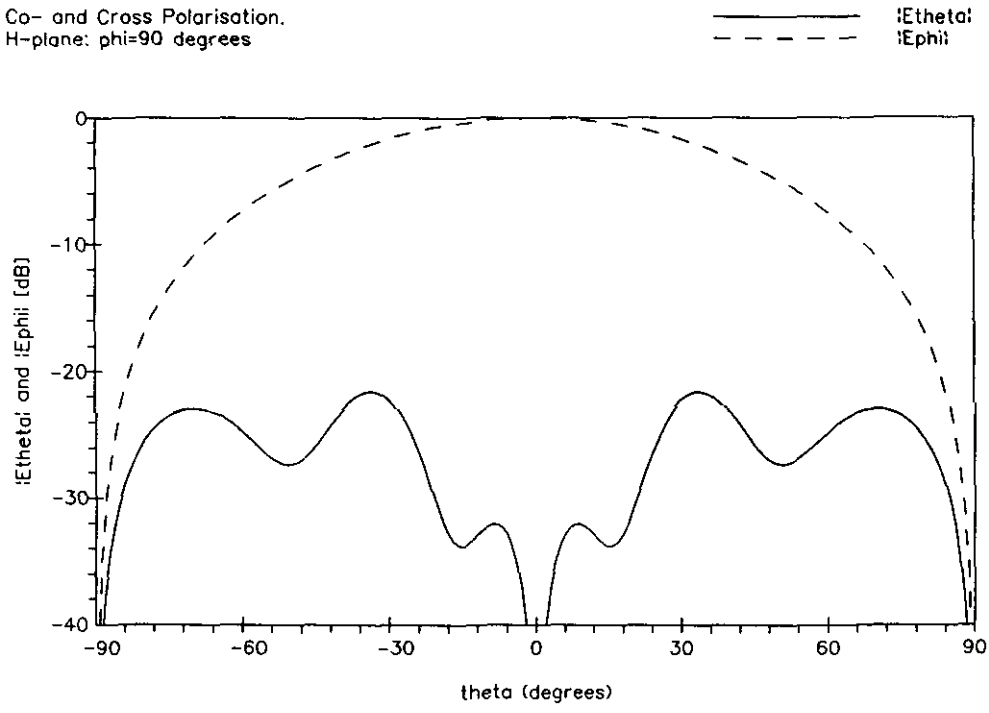

Figure 3.6: Calculated H-plane radiation pattern, f=6.9 GHz

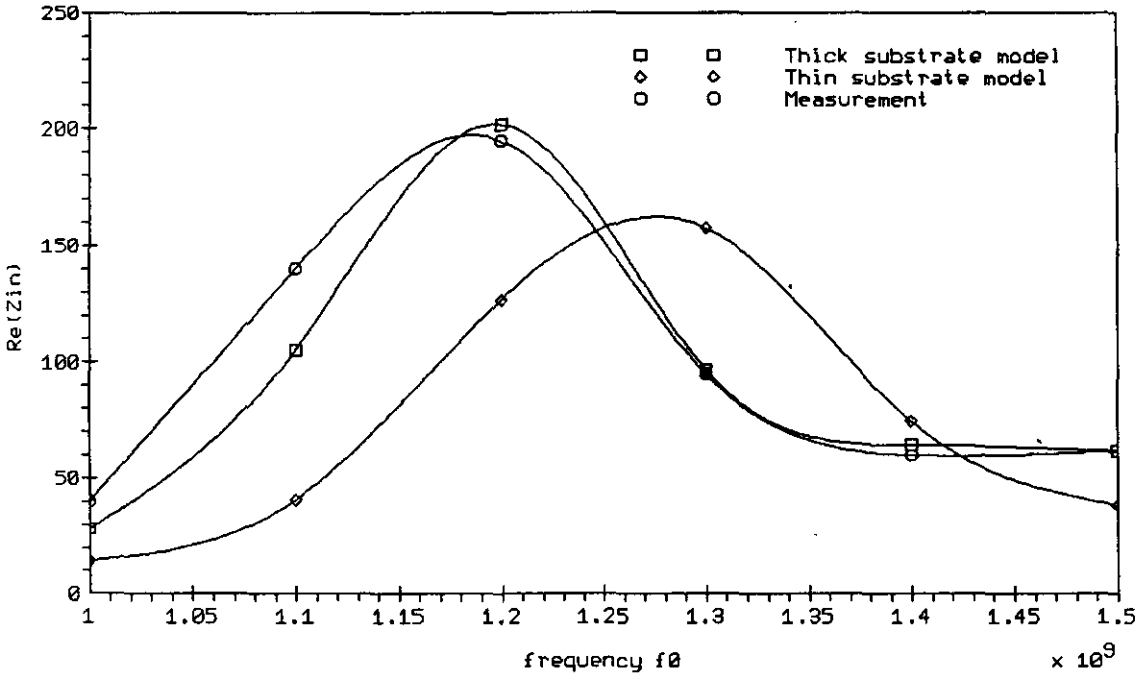

Figure 3.7: Real part of input impedance (measured and calculated)

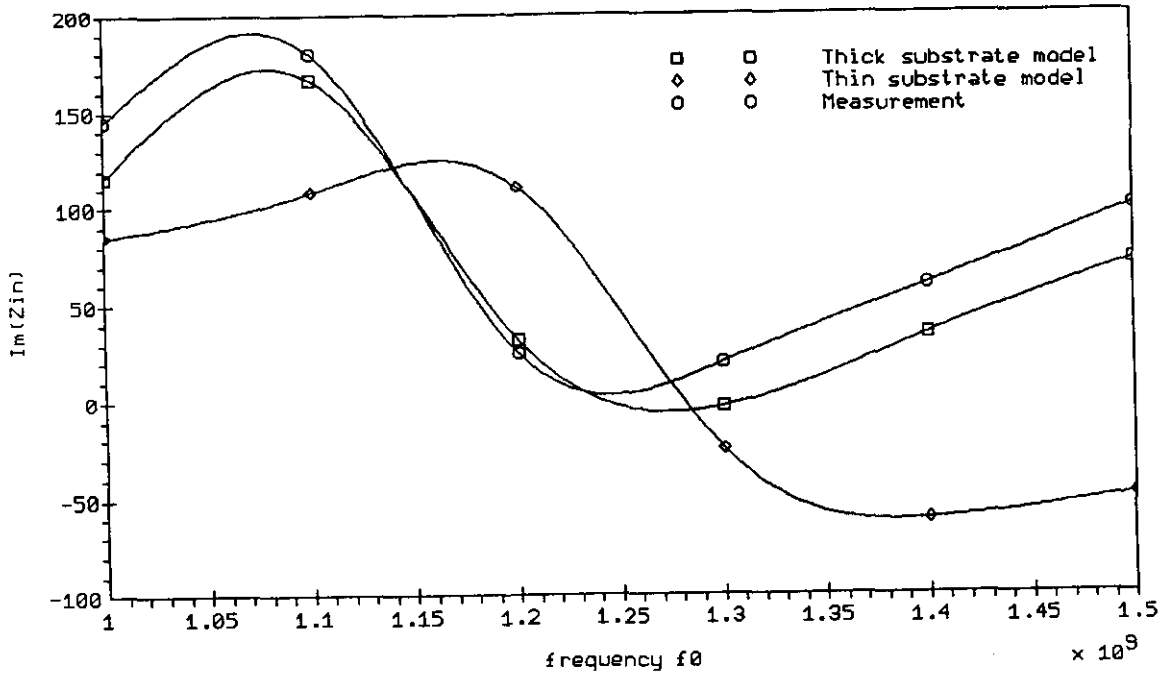

Figure 3.8: Imaginary part of input impedance (measured and calculated)

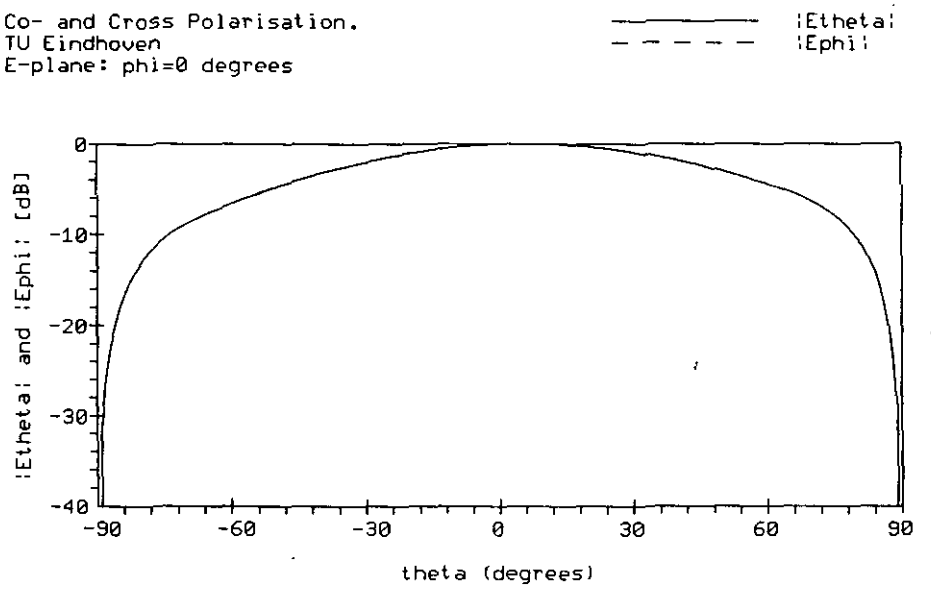

Figure 3.9: Calculated E-plane radiation pattern, f=1.2 GHz

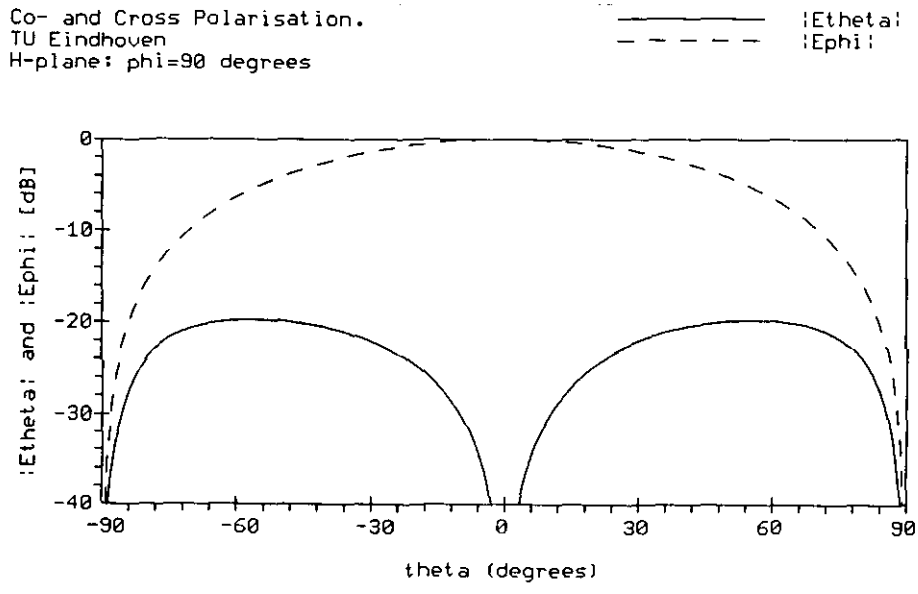

Figure 3.10: Calculated H-plane radiation pattern, f=1.2 GHz

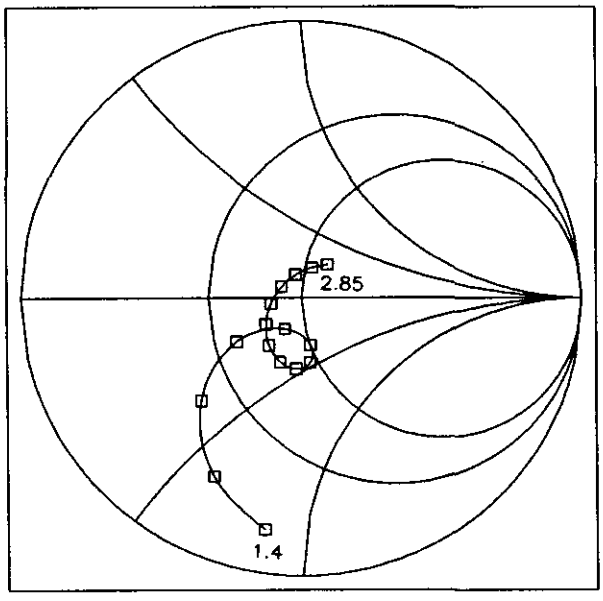

Figure 3.11: Input impedance of EMC coupled microstrip antenna

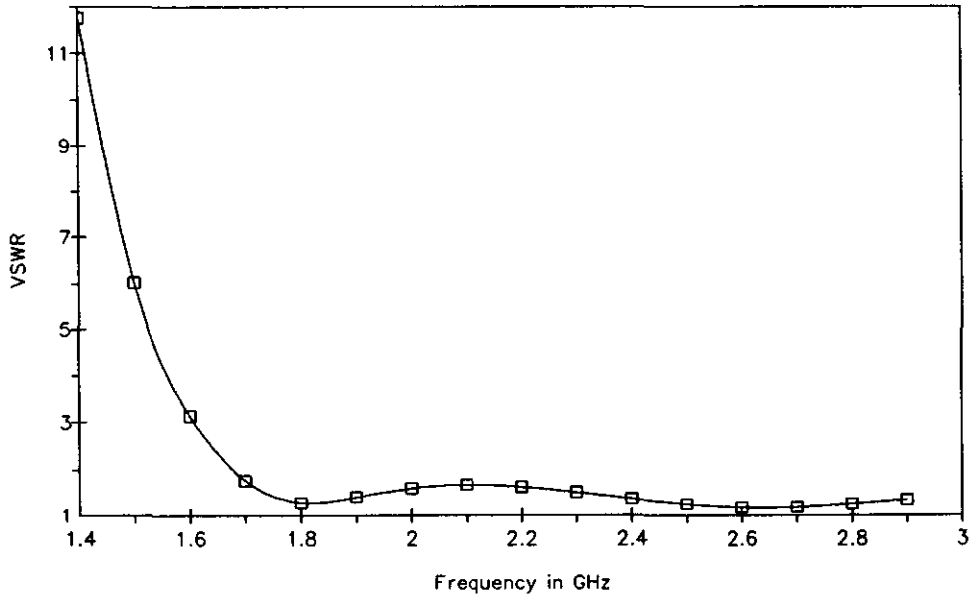

Figure 3.12: VSWR ratio of EMC coupled microstrip antenna

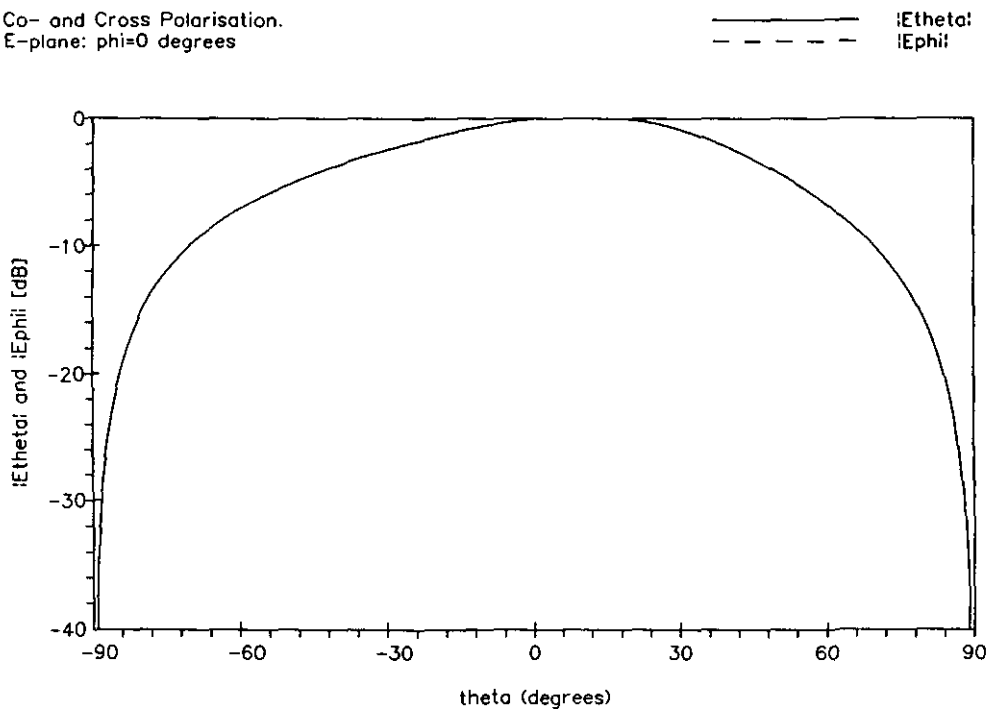

Figure 3.13: E-plane pattern of EMC coupled microstrip antenna, f=2 GHz

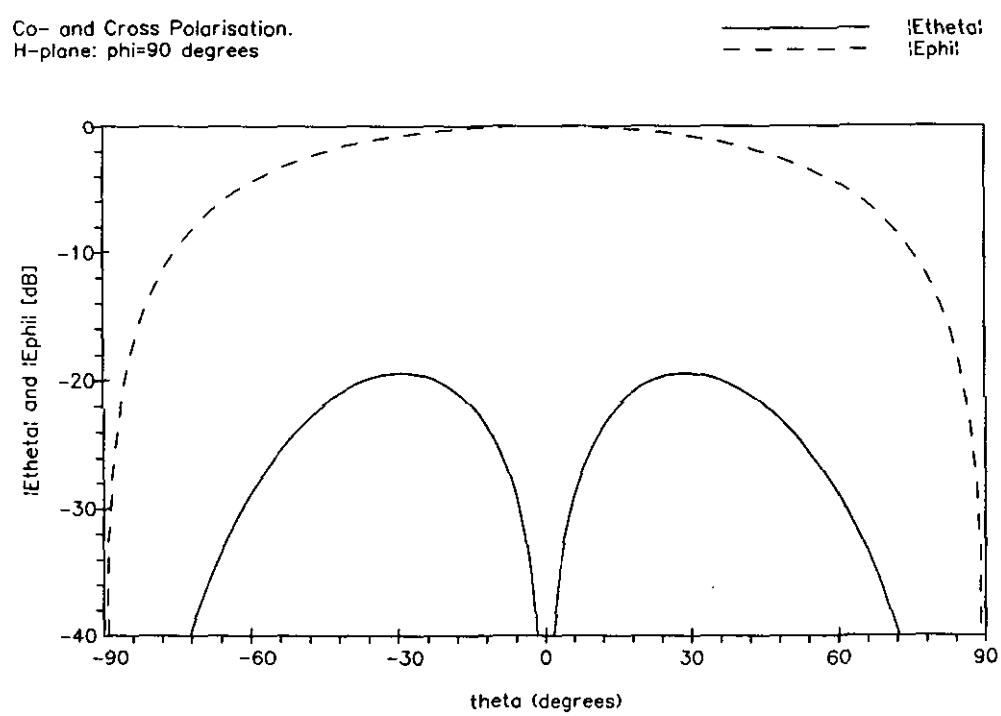

Figure 3.14: H-plane pattern of EMC coupled microstrip antenna, f=2 GHz

Chapter 4

Radiation pattern of thick microstrip antennas

4.1 Far field pattern

After applying the method of moments we have an approximation for the currents on the patch and on the feeding coaxial probe. The easiest way to determine the far field pattern is to use Huygens' principle. This means that the sources in the dielectric substrate are replaced by an equivalent electric and magnetic current distribution on the upper surface of the substrate, denoted S (see figure 4.1) . This can be simplified if we assume that the infinite plane S is a perfect electric conductor. In this case only the equivalent magnetic current remains and is given by:

$$\vec{J}_m = \vec{\mathcal{E}} \times \vec{n} = \vec{\mathcal{E}} \times \vec{e}_z \tag{4.1}$$

We can eliminate the presence of the perfectly conducting infinite plane S by applying image theory, i.e. replace $\vec{J}_m$ by $2\vec{J}_m$ and remove the perfectly conducting plane. A relation between the tranversal electric fields in the dielectric layer and the vector potential at the point $\vec{r} = (x, y, z)$ in free space is given by [2]:

$$\vec{A}(\vec{r}) = \frac{\epsilon_0}{4\pi} \int\int\int_V 2\vec{J}_m \frac{e^{jk_0|\vec{r}-\vec{r}_0|}}{|\vec{r}-\vec{r}_0|} dr_0 \tag{4.2}$$

Note that $\vec{r}_0 = (x_0, y_0, z_0)$ represents a source point and V_0 is the volume enclosing the source currents. In the far field region where $|\vec{r}| \gg |\vec{r}_0|$ the electic field is given by:

$$\vec{\mathcal{E}}(\vec{r}) = \frac{jk_0 e^{-jk_0 r}}{4\pi r} \vec{e}_r \int\int_S 2\vec{J}_m(x_0, y_0, d) e^{jk_0 \vec{e}_r . \vec{r}_0} dx_0 dy_0 \tag{4.3}$$

$\vec{e}_r$ is an unit vector in the $\vec{r}$ direction. Far fields are usually expressed in terms of spherical coordinates (r, θ, ϕ) instead of cartesian coordinates (x, y, z). The coordinate system is defined in figure 4.2.
The dot-product $\vec{e}_r.\vec{r}_0$ can be written in the form:

$$\vec{e}_r.\vec{r}_0 = \frac{xx_0 + yy_0 + zz_0}{r} = x_0 \sin\theta\cos\phi + y_0 \sin\theta \sin\phi + z_0 \cos\theta \tag{4.4}$$

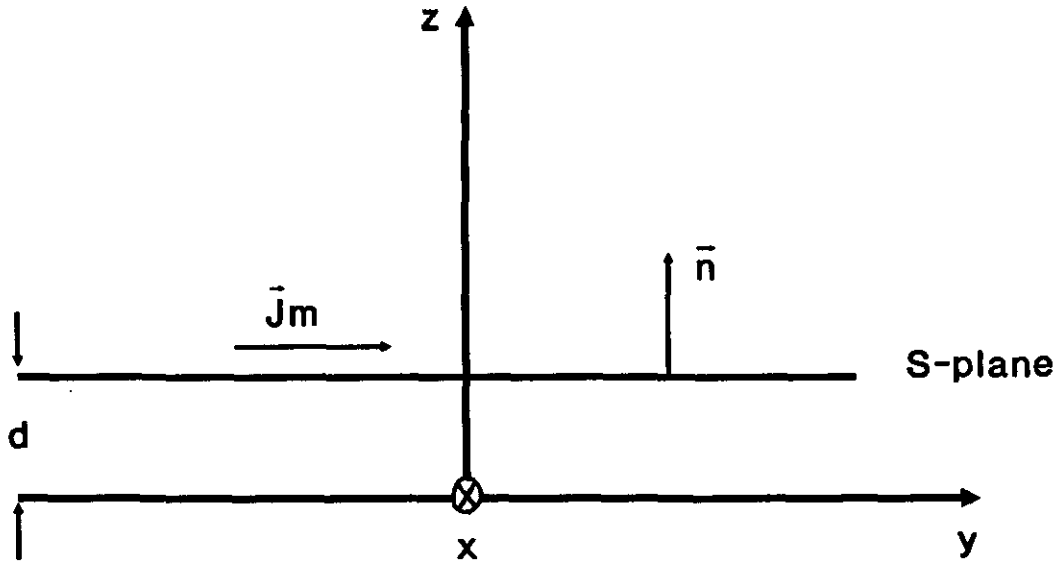

Figure 4.1: Equivalent magnetic current source

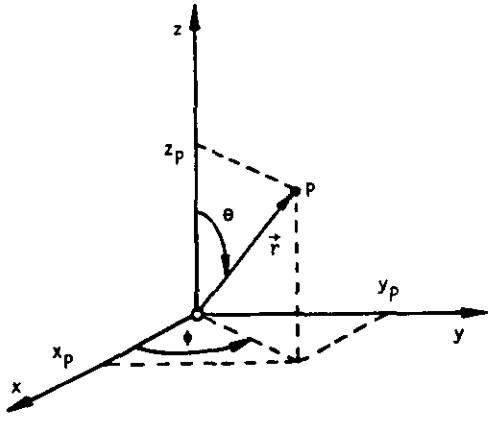

Figure 4.2: Coordinate system

Combining equation (4.3) with this last expression results in:

$$\begin{aligned}\vec{\mathcal{E}}(\vec{r}) = \; & \frac{jk_0e^{-jk_0r}}{4\pi r}e^{jk_0d\cos\theta}\vec{e}_r\times \\ & \int\int_S 2\vec{\mathcal{J}}_m(x_0,y_0,d)e^{jk_0(x_0\sin\theta\cos\phi+y_0\sin\theta\sin\phi)}dx_0dy_0\end{aligned} \tag{4.5}$$

Now let $k_x = k_0\sin\theta\cos\phi$ and $k_y = k_0\sin\theta\sin\phi$. The integral over S in (4.5) can then be written in terms of the spectral domain electric field:

$$\begin{aligned}&\int\int_S \vec{\mathcal{J}}_m(x_0,y_0,d)e^{jk_0(k_xx_0+k_yy_0)}dx_0dy_0 \\ &= \int_{-\infty}^{\infty}\int_{-\infty}^{\infty}[\vec{\mathcal{E}}(x_0,y_0,d)\times\vec{e}_z]e^{jk_0(k_xx_0+k_yy_0)}dx_0dy_0 \\ &= \vec{E}(k_x,k_y,d)\times\vec{e}_z\end{aligned} \tag{4.6}$$

Using this important result, the far field can be expressed in a closed form expression:

$$\begin{aligned}\vec{\mathcal{E}}(\vec{r}) \; &= \frac{jk_0e^{-jk_0r}}{2\pi r}e^{jk_0d\cos\theta} \quad \vec{e}_r\times[\vec{E}(k_x,k_y,d)\times\vec{e}_z] \\ &= \frac{jk_0e^{-jk_0r}}{2\pi r}e^{jk_0d\cos\theta} \quad [\vec{e}_\phi(E_y\cos\theta\cos\phi - E_x\cos\theta\sin\phi) \\ &\qquad\qquad\qquad\qquad +\vec{e}_\theta(E_y\sin\phi + E_x\cos\phi)]\end{aligned} \tag{4.7}$$

With $k_x = k_0\sin\theta\cos\phi$, $k_y = k_0\sin\theta\sin\phi$ and $\vec{E} = E_x\vec{e}_x + E_y\vec{e}_y$. The electric field in the spectral domain can be written in terms of the current distribution on the patch and feeding probe in the spectral domain. At the plane $z_0 = d$ the spectral domain electric field is according to (3.1) given by:

$$\begin{aligned}\vec{E}(k_x,k_y,d) = \; & \bar{\bar{Q}}(k_x,k_y,z',d).\vec{J}_{patch}(k_x,k_y,z') \\ & + \int_0^{z'}\bar{\bar{Q}}(k_x,k_y,z_0,d).\vec{J}_{feed}(k_x,k_y,z_0)dz_0\end{aligned} \tag{4.8}$$

Note that we have neglected the magnetic current source in the coaxial aperture in the above expression. Because an approximation of $\vec{J}_{patch}$ and $\vec{J}_{feed}$ is known in terms of expansion functions, the far field pattern can be calculated very easily with (4.7). Note that the z-integration in (4.8) can be calculated analytically. The corresponding magnetic field in the far field region can also be determined by using the relation:

$$\vec{\mathcal{H}} = \sqrt{\frac{\mu_0}{\epsilon_0}}\vec{e}_z\times\vec{\mathcal{E}} \tag{4.9}$$

4.2 Circular polarization

The far field pattern derived in the previous section is essentially a linear polarized field, because we only considered one feedpoint for the microstrip antenna. Using two feeding probes with a 90 degree phase difference, a circular polarized far field pattern can be obtained at broadsight ($\theta = \phi = 0$). For other angles the polarization of the far field will be elliptical. The electric far field can now be divided in two components, i.e. a Right Hand Circularly polarized wave (RHC) and a Left Hand Circularly polarized wave (LHC):

$$\begin{aligned} \vec{\mathcal{E}} &= E_\theta \vec{e}_\theta + E_\phi \vec{e}_\phi \\ &= E_L \vec{e}_L + E_R \vec{e}_R \end{aligned} \tag{4.10}$$

With

$$\vec{e}_L = \frac{1}{\sqrt{2}}(\vec{e}_\theta + j\vec{e}_\phi)$$
$$\vec{e}_R = \frac{1}{\sqrt{2}}(\vec{e}_\theta - j\vec{e}_\phi)$$

and

$$E_L = \frac{1}{\sqrt{2}}(E_\theta - jE_\phi)$$
$$E_R = \frac{1}{\sqrt{2}}(E_\theta + jE_\phi)$$

E_L is the LHC component and E_R the RHC component of the wave. If one of these two components is zero, the far field is perfectly circularly polarized. A quantity that can be used to describe the polarization mismatch is the axial ratio (AR). The axial ratio is defined by:

$$AR = \left| \frac{|E_L| + |E_R|}{|E_L| - |E_R|} \right| \tag{4.11}$$

The axial ratio is used here to describe the polarization mismatch , because this quantity is easy to measure.

Chapter 5

Conclusion

Electrically thick microstrip antennas, fed by a coaxial cable, can be analyzed using a spectral domain moment method with a proper model for the feeding coaxial structure and by incorporating the current continuity at the patch-coax transition. A special attachment mode is used at this transition to describe the current distribution in an accurate way. The efficiency of the method of moments can be significantly improved by using the source term extraction technique, where a great part of the infinite integrals involved with the method of moment formulation is calculated analytically. Computing time can also be saved by selecting a set of basis functions that describes the current distribution on the patch and probe in an accurate way, using only a few terms of this set.

Electrically thick microstrip antennas have broadband characteristics. However, a proper match to 50 Ω is often difficult to achieve due to an inductive shift in the input impedance. Another microstrip structure is proposed in order to avoid this matching problem. The patch is now electromagnetically coupled to the coaxial probe. With this antenna a bandwidth of more than 40 percent can easily be obtained. The radiation pattern of this antenna is somewhat asymmetrical and the cross polarisation level is deteriorated. Therefore more research has to be performed on this type of microstrip antenna.

Bibliography

[1] Smolders A.B.
ANALYSIS OF MICROSTRIP ANTENNAS IN THE SPECTRAL DOMAIN USING A MOMENT METHOD.
Professional group Electromagnetism, Faculty of Electrical Engineering,
Eindhoven University of Technology, The Netherlands, 1989.
M. Sc. Thesis, divisional no. ET-15-89.

[2] Harrington R.F.
TIME HARMONIC FIELDS.
New York: McGraw-Hill, 1961.

[3] Mosig J.R. and F.E. Gardiol
A DYNAMICAL RADIATION MODEL FOR MICROSTRIP ANTENNAS.
In: Advances in Electronics and Electron Physics, by P. Hawkes.
New York: Academic Press, 1982, Vol. 59, p. 139-237.

[4] Smolders, A.B.
AN EFFICIENT METHOD FOR ANALYZING MICROSTRIP ANTENNAS WITH A DIELECTRIC COVER USING A SPECTRAL DOMAIN MOMENT METHOD.
Eindhoven: Faculty of Electrical Engineering,
Eindhoven University of Technology, 1991.
EUT Report 91-E-255.

[5] Gradsteyn, I.S. and I.M. Ryzhik
TABLE OF INTEGRALS, SERIES AND PRODUCTS.
New York: Academic Press, 1965.

[6] Hall, R.C. and J.R. Mosig
VERTICAL MONOPOLES EMBEDDED IN A DIELECTRIC SUBSTRATE.
IEE Proceedings-H, Vol. 136 (1989), p. 462-468.

[7] Pozar, D.M.
INPUT IMPEDANCE AND MUTUAL COUPLING OF RECTANGULAR MICROSTRIP ANTENNAS.
IEEE Trans. on Antennas and Propagation, vol. AP-30 (1982), p.1191-1196.

[8] Gronau, G.
THEORETISCHE UND EXPERIMENTELLE UNTERSUCHUNG DER VERKOPPLUNG IN STREIFENLEITUNGSANTENNEN.
Ph.D. Thesis, Duisburg University, Germany, 1987.

[9] Hall R.C. and J.R. Mosig
THE ANALYSIS OF COAXIALLY FED MICROSTRIP ANTENNAS WITH ELECTRICALLY THICK SUBSTRATES.
Electromagnetics, vol. 9 (1989), p. 367-384.

[10] Pozar D.M.
ANALYSIS OF INFINITE ARRAYS OF PROBE-FED RECTANGULAR MICROSTRIP ANTENNAS USING A RIGOROUS FEED MODEL.
IEE Proceedings-H, vol. 136 (1989), p. 110-119.

[11] Shaeffer J.F. and L.N. Medgyesi-Mitschang
RADIATION FROM WIRE ANTENNAS ATTACHED TO BODIES OF REVOLUTION: THE JUNCTION PROBLEM.
IEEE Trans. on Antennas and Propagation, vol. AP-29 (1981), p.479-487.

[12] Carver K.R. and J.W. Mink
MICROSTRIP ANTENNA TECHNOLOGY.
IEEE Trans. on Antennas and Propagation, vol. AP-29 (1981), p.2-24.

[13] Chang E. and S.A. Long, W.F. Richards
AN EXPERIMENTAL INVESTIGATION OF ELECTRICALLY THICK RECTANGULAR MICROSTRIP ANTENNAS.
IEEE Trans. on Antennas and Propagation, vol. AP-34 (1986), p.767-772.

Eindhoven University of Technology Research Reports ISSN 0167-9708
Coden: TEUEDE

Faculty of Electrical Engineering

(238) Lammers, J.O.
THE USE OF PETRI NET THEORY FOR SIMPLEXYS EXPERT SYSTEMS PROTOCOL CHECKING.
EUT Report 90-E-238. 1990. ISBN 90-6144-238-9

(239) Wang, X.
PRELIMINARY INVESTIGATIONS ON TACTILE PERCEPTION OF GRAPHICAL PATTERNS.
EUT Report 90-E-239. 1990. ISBN 90-6144-239-7

(240) Lutgens, J.M.A.
KNOWLEDGE BASE CORRECTNESS CHECKING FOR SIMPLEXYS EXPERT SYSTEMS.
EUT Report 90-E-240. 1990. ISBN 90-6144-240-0

(241) Brinker, A.C. den
A MEMBRANE MODEL FOR SPATIOTEMPORAL COUPLING.
EUT Report 90-E-241. 1990. ISBN 90-6144-241-9

(242) Kwaspen, J.J.M. and H.C. Heyker, J.I.M. Demarteau, Th.G. van de Roer
MICROWAVE NOISE MEASUREMENTS ON DOUBLE BARRIER RESONANT TUNNELING DIODES.
EUT Report 90-E-242. 1990. ISBN 90-6144-242-7

(243) Massee, P. and H.A.L.M. de Graaf, W.J.M. Balemans, H.G. Knoopers, H.H.J. ten Kate
PREDESIGN OF AN EXPERIMENTAL (5-10 MWt) DISK MHD FACILITY AND PROSPECTS OF COMMERCIAL (1000 MWt) MHD/STEAM SYSTEMS.
EUT Report 90-E-243. 1990. ISBN 90-6144-243-5

(244) Klompstra, Martin and Ton van den Boom, Ad Damen
A COMPARISON OF CLASSICAL AND MODERN CONTROLLER DESIGN: A case study.
EUT Report 90-E-244. 1990. ISBN 90-6144-244-3

(245) Berg, P.H.G. van de
ON THE ACCURACY OF RADIOWAVE PROPAGATION MEASUREMENTS: Olympus propagation experiment.
EUT Report 90-E-245. 1990. ISBN 90-6144-245-1

(246) Maagt, P.J.I. de
A SYNTHESIS METHOD FOR COMBINED OPTIMIZATION OF MULTIPLE ANTENNA PARAMETERS AND ANTENNA PATTERN STRUCTURE.
EUT Report 90-E-246. 1990. ISBN 90-6144-246-X

(247) Józwiak, L. and T. Spassova-Kwaaitaal
DECOMPOSITIONAL STATE ASSIGNMENT WITH REUSE OF STANDARD DESIGNS: Using counters as sub-machines and using the method of maximal adjacensies to select the state chains and the state codes.
EUT Report 90-E-247. 1990. ISBN 90-6144-247-8

(248) Hoeijmakers, M.J. and J.M. Vleeshouwers
DERIVATION AND VERIFICATION OF A MODEL OF THE SYNCHRONOUS MACHINE WITH RECTIFIER WITH TWO DAMPER WINDINGS ON THE DIRECT AXIS.
EUT Report 90-E-248. 1990. ISBN 90-6144-248-6

(249) Zhu, Y.C. and A.C.P.M. Backx, P. Eykhoff
MULTIVARIABLE PROCESS IDENTIFICATION FOR ROBUST CONTROL.
EUT Report 91-E-249. 1991. ISBN 90-6144-249-4

(250) Pfaffenhofer, F.M. and P.J.M. Cluitmans, H.M. Kuipers
EMDABS: Design and formal specification of a datamodel for a clinical research database system.
EUT Report 91-E-250. 1991. ISBN 90-6144-250-8

Eindhoven University of Technology Research Reports ISSN 0167-9708
Coden: TEUEDE

Faculty of Electrical Engineering

(251) Eijndhoven, J.T.J. van and G.G. de Jong, L. Stok
THE ASCIS DATA FLOW GRAPH: Semantics and textual format.
EUT Report 91-E-251. 1991. ISBN 90-6144-251-6

(252) Chen, J. and P.J.I. de Maagt, M.H.A.J. Herben
WIDE-ANGLE RADIATION PATTERN CALCULATION OF PARABOLOIDAL REFLECTOR ANTENNAS: A comparative study.
EUT Report 91-E-252. 1991. ISBN 90-6144-252-4

(253) Haan, S.W.H. de
A PWM CURRENT-SOURCE INVERTER FOR INTERCONNECTION BETWEEN A PHOTOVOLTAIC ARRAY AND THE UTILITY LINE.
EUT Report 91-E-253. 1991. ISBN 90-6144-253-2

(254) Velde, M. van de and P.J.M. Cluitmans
EEG ANALYSIS FOR MONITORING OF ANESTHETIC DEPTH.
EUT Report 91-E-254. 1991. ISBN 90-6144-254-0

(255) Smolders, A.B.
AN EFFICIENT METHOD FOR ANALYZING MICROSTRIP ANTENNAS WITH A DIELECTRIC COVER USING A SPECTRAL DOMAIN MOMENT METHOD.
EUT Report 91-E-255. 1991. ISBN 90-6144-255-9

(256) Backx, A.C.P.M. and A.A.H. Damen
IDENTIFICATION FOR THE CONTROL OF MIMO INDUSTRIAL PROCESSES.
EUT Report 91-E-256. 1991. ISBN 90-6144-256-7

(257) Maagt, P.J.I. de and H.G. ter Morsche, J.L.M. van den Broek
A SPATIAL RECONSTRUCTION TECHNIQUE APPLICABLE TO MICROWAVE RADIOMETRY
EUT Report 92-E-257. 1992. ISBN 90-6144-257-5

(258) Vleeshouwers, J.M.
DERIVATION OF A MODEL OF THE EXCITER OF A BRUSHLESS SYNCHRONOUS MACHINE.
EUT Report 92-E-258. 1992. ISBN 90-6144-258-3

(259) Orlov, V.B.
DEFECT MOTION AS THE ORIGIN OF THE 1/F CONDUCTANCE NOISE IN SOLIDS.
EUT Report 92-E-259. 1992. ISBN 90-6144-259-1

(260) Rooijackers, J.E.
ALGORITHMS FOR SPEECH CODING SYSTEMS BASED ON LINEAR PREDICTION.
EUT Report 92-E-260. 1992. ISBN 90-6144-260-5

(261) Boom, T.J.J. van den and A.A.H. Damen, Martin Klompstra
IDENTIFICATION FOR ROBUST CONTROL USING AN H-infinity NORM.
EUT Report 92-E-261. 1992. ISBN 90-6144-261-3

(262) Groten, M. and W. van Etten
LASER LINEWIDTH MEASUREMENT IN THE PRESENCE OF RIN AND USING THE RECIRCULATING SELF HETERODYNE METHOD.
EUT Report 92-E-262. 1992. ISBN 90-6144-262-1

(263) Smolders, A.B.
RIGOROUS ANALYSIS OF THICK MICROSTRIP ANTENNAS AND WIRE ANTENNAS EMBEDDED IN A SUBSTRATE.
EUT Report 92-E-263. 1992. ISBN 90-6144-263-X